

28TH ANNUAL EUROPEAN
MEETING ON ATMOSPHERIC STUDIES BY
OPTICAL METHODS

PROGRAMME, ABSTRACTS AND INFORMATION

August 19th – 24th, 2001
Oulu, Finland

Space Physics Group of University of Oulu

CONTENTS

- Conference Programme
- Abstracts:
 - Session 1: Auroral physics and other Ionospheric phenomena
 - Session 2: Auroral observations monitoring magnetospheric phenomena and Space born studies
 - Session 3: Odin; The first results
 - Session 4: Tropospheric and Stratospheric physics
 - Session 5: Mesospheric and Thermospheric physics
 - Session 6: Techniques, Methods and Instrumentation
 - Session 7: Calibration
- Participants list
- Information

Cover page picture:

Thomas Ulich and Petri Kekkonen (the more freezing one)
photographing a bright, rayed arc in Oulu, 19th March 2001 ~21 UT.
– Jouni Jussila

CONFERENCE PROGRAMME

SUNDAY 19TH AUGUST

- 10.00 Registration
- 11.00 Start to Kierikki archeological centre.
- 20.00 Ice-breaking party at POHTO (incl.sauna)

MONDAY 20TH AUGUST

- 08.30 Registration
- 09.00 Welcome to the participants and practical information

Session Ia: Auroral physics and other ionospheric phenomena (Chairperson Kari Kaila)

- 09.30 O1.1: **Lummerzheim, D. et al.**, Optical Emissions from Proton Aurora (invited).
- 10.00 O1.2: **Kosch M**, High Latitude Artificial Aurora from HEATING: A Unique Phenomenon? (Invited).
- 10.30 Coffee break
- 11.00 O1.3: **Donovan, E. et al.**, Energy Dependence of the Latitude of the Equatorward Edge of Significant Proton Auroral Precipitation.
- 11.20 O1.4: **Sergienko, T. et al.**, Study of auroral arc fine structure with conjugate FAST and ALIS measurements.
- 11.40 O1.5: **Leontyev, S.V.**, Neutral winds in the e-layer of auroral zone during quiet and disturbed conditions.
- 12.00 Lunch break

Session Ib: Auroral physics and other ionospheric phenomena (Chairperson Kirsti Kauristie)

- 13.10 O1.6: **Safargaleev, V. et al.**, Multiple Poleward Propagating Auroral Events in the 15-16 MLT Sector.
- 13.30 O1.7: **Kozlovsky, A.**, Characteristics of the Noon Poleward Moving Auroral Arcs Inferred from EISCAT Radar Measurements.
- 13.50 O1.8: **Pitkänen V. et al.**, Ground-Based Optical Observations of Dayside Aurora at Zhong Shan Station in Antarctic.
- 14.10 O1.9: **Lyatsky, W.**, Auroral Phenomena as Seen from Spacecraft Auroral UV Images (a review).
- 14.30 Coffee break
- 15.00 O1.10: **Ulich, T. et al.**, Modelling of Pulsating Aurora Observed by EISCAT with the Detailed Sodankylä Ion-Neutral Chemistry Model.
- 15.20 O1.11: **Tagirov, V. et al.**, TV observations of auroral forms at different zones of high latitudes (review).
- 15.40 O1.12: **Danielides, M. et al.**, Cosmic Radio Noise Absorption Associated with North-South Aurora.
- 16.00 O1.13: **Kozelov, B. et al.**, Visualization of Physical Processes Related to Combined Electron-Proton Aurorae. Software for Science and Education.

TUESDAY 21ST AUGUST

Session Ic: Auroral physics and other ionospheric phenomena (Chairperson Hannu Holma)

- 09.00 O1.14: **Lyatsky, W. and Hamza, A. M.**, Auroral Arc and Substorm Generation: Theory and Observations (a review). (invited)
- 09.30 O1.15: **Lummerzheim, D. et al.**, Preliminary Results of Observations Acquired with the Hittes Spectrograph on Svalbard: The H β Line Profile, The 1NG (1,3) Band and the OII Multiplet (4P-4D)
- 09.50 O1.16: **Laine, U. K. et al.**, Auroral Sounds, Observations and Measurements
- 10.10 Coffee break

Session II: Auroral observations monitoring magnetospheric phenomena and Space borne studies (Chairperson Vartan Tagirov)

- 10.40 O2.1: **Aikio, A.**, Electrodynamics of auroral arcs. (invited)
- 11.10 O2.2: **Moen, J.**, Auroral signatures of dayside boundary layer dynamics. (invited)
- 11.40 O2.3: **Amm, O.**, Analysis of auroral signatures and electrodynamics of a pseudobreakup event, using observations of the MIRACLE network
- 12.00 Lunch break
- 13.10 O2.4: **Nicholson, N. et al.**, Monitoring the Ion Isotropy Boundary with Multipoint Proton Auroral Measurements.
- 13.30 O2.5: **Kornilov, I.A. et al.**, Using image filtering methods for TV data processing: Subvisual auroral wave structures and pulsations.
- 13.50 O2.6: **Starkov, G. et al.**, HF Radar observations of Auroral Boundaries.
- 14.10 O2.7: **Kauristie, K. et al.**, Ground-based and satellite observations of high-latitude auroral activity in the dusk sector of the auroral oval.
- 14.30 Coffee break

Session III: Odin; The first results (Chairperson Gilbert Leppelmeier)

- 15.00 O3.1: **Murtagh D.**, An Overview of the Odin Aeronomy Science Program and First Results (invited)
- 15.30 O3.2: **Llewellyn, E. J.**, First Results from the OSIRIS Instrument on-board Odin (invited)
- 16.00 O3.3: **Degenstein, D.**, The Incorrect Interpretation of Atmospheric Images as seen with OSIRIS.
- 16.20 O3.4: **Murtagh D.**, Early results from the Sub-MM Radiometer onboard Odin.

- 19.00 Conference Sauna

WEDNESDAY 22ND AUGUST

Session IV: Tropospheric and Stratospheric physics (Chairperson Edward Llewellyn)

- 09.00 O4.1: **Leppelmeier, G. W.**, Atmospheric Research on Envisat. (invited)
09.30 O4.2: **Enell, C.-F. et al.**, Detecting polar stratospheric clouds using the zenith-sky colour index.
09.50 Coffee break

Session Va: Mesospheric and Thermospheric physics (Chairperson Donal Murtaugh)

- 10.30 O5.1: **Grossmann, K. U. et al.**, Upper mesosphere/ lower thermosphere measurements by CRISTA. (invited)
11.00 O5.2: **Oldag, J. et al.**, Temperatures and Semidiurnal Tides in The Mesopause Region at 54°N And 28°N Latitude by Potassium Lidar. (invited)
11.30 Lunch break
(Operational manager J. Koivukoski: Introduction to POHTO Training factory for electronic industry)
13.10 O5.3: **Lowe R. P.**, Gravity Wave Measurements with a Near Infrared Scanning Radiometer at ALOMAR.
13.50 O5.4: **Kirillov, A. S.**, Application of Quantum-Chemical Approximations in the Calculation of Rate Coefficients for Intramolecular and Intermolecular Energy Transfer Processes of Atmospheric Gases.
14.10 Coffee break

Session Vb: Mesospheric and Thermospheric physics (Chairperson Esa Turunen)

- 14.40 O5.5: **López-Moreno J. J.**, Extreme Ultraviolet Airglow. (invited)
15.10 O5.6: **Sigernes F.**, The Hydroxyl Rotational Temperature Record from the Auroral Station in Adventdalen, Svalbard (78N,15E). (invited)
15.40 O5.7: **Witt G.**, IR and thermal properties of mesospheric particles (invited)
16.10 O5.8: **Sivjee, G.G. and** McEwen, D. J., Polar cap Disturbances: Mesosphere and Thermosphere-Ionosphere Response to Solar-Terrestrial Interactions.

19.00 Conference Dinner

THURSDAY 23RD AUGUST

Session VI: Techniques, Methods and Instrumentation (Chairperson Michael Kosch)

- 09.00 O6.1: **Janhunen, P.**, Inversion of electron fluxes from all-sky images. (Invited)
- 09.30 O6.2: **Arinin V. A. and Tagirov V.R.**, New Method for Study of Aurora Brightness Spatial Distribution.
- 09.50 O6.3: **Syrjäso, M.T et al.**, Can computers understand auroral images?
- 10.10 O6.4: **McWhirter, I. et al.**, A new spectrograph platform for auroral studies in Svalbard.
- 10.30 Coffee break
- 11.00 O6.5: **Robertson S.**, Development of an Online Field Aligned Support Imager for the ESR.
- 11.20 O6.6: **Borovkov, L. and Chernouss, S.**, Application of the I-PentaMAX CCD camera for auroral observations.
- 11.40 O6.7: **Gausa, M. et al.**, DIAL Measurements of Stratospheric Ozone.
- 12.00 O6.8: **Enell, C.-F. et al.**, Bistatic stereoscopy in studies of polar stratospheric clouds.
- 12.20 Lunch break
- 13.30 O6.9: **Widell O.**, Ground Based Instrumentation at ESRange.
- 13.50 O6.10: **Jussila J. et al.**, Optical auroral instrumentation of University of Oulu.
- 14.10 O6.11: **Sigernes F. et al.**, OPTICS at the Auroral Station in Adventdalen, Svalbard.

Session VII: Calibration (Chairperson Kari Kaila)

- 14.40 O7.1: **Mäkinen, S.**, All-sky camera calibration. (Invited)
- 15.00 O7.2: **Brändström, U. et al.**, Calibration of an Auroral Large Imaging System.
- 15.20 Conference Closing
- 15.30 Coffee

FRIDAY 24TH AUGUST

- 09.00 - 15.00 Calibration workshop at the University of Oulu

POSTERS

- P1.1: *Yevlashin, L. and Chernouss, S.*, The Red Type-A Auroras during Superstorms Caused by Coronal Mass Ejection (CMEs)
- P1.2: *Donovan, Eric et al.*, Triangulation of auroral red-line emissions
- P1.3: *Kornilova, T.*, Auroral Pulsations in Diffuse Luminosity During Substorm
- P1.4: *Kaila K. U. et al.*, Auroral Structures and Emissions in the Antarctic
- P1.5: *Holma H. et al.*, Particle energy estimations in the quiet arc.
-
- P2.1: *Kornilov, I.A.*, Fine details of space and time structure of pulsating aurora and VLF-chorus emissions
- P2.2: *Kornilov, I.A. et al.*, Using image filtering methods for TV data processing: Subvisual auroral wave structures and pulsations
- P2.3: *Donovan, E. et al.*, All-Sky Imaging Within the Canadian CANOPUS and NORSTAR Projects
- P2.4: *Kozelov, B.V. and Kozelova, T.V.*, Developing of auroral intensification as an output of magnetosphere-ionosphere dynamical system
- P2.5: *Safargaleev, V. et al.*, Azimuthal Propagation of the Auroral Arcs
- P2.6: *Yahnin, A.G. et al.*, Auroral Breakup As Observed From Above And Below: Multi-Instrument Case Study
- P2.7: *Oikarinen A.*, Ionospheric heating at Tromsø – Source for active space experiments
-
- P4.1: *Milnevsky, G. et al.*, Cloudiness and Divergence Between Ground-Based and Satellite Total Ozone Measurements
- P4.2: *Milnevsky, G. et al.*, The Changes of Total Ozone Over Antarctic Peninsula and Ukraine for 1996-2001
- P4.3: *Roldugin, V.C.*, Invariability of Total Ozone Content Under Solar Proton Events
- P4.4: *Roldugin, V.C. and Tinsley, B.A.*, Changes of Atmospheric Aerosol Density After Earth Transits of the Heliospheric Current Sheet.
-
- P5.1: *Kirillov, A. S.*, The Study of the Role of Collisional Processes in Electronic Kinetics of Singlet and Triplet States of Molecular Nitrogen in High-Latitude Upper and Middle Atmosphere
- P5.2: *Aushev, V.M. et al.*, A spectrum of atmospheric gravity waves in the mesosphere and thermosphere.
-
- P6.1: *Rydesäter P. et al.*, Lossy compression of scientific images of aurora
- P6.2: *McWhirter, I. et al.*, Neutral wind and temperature measurements from the University College London Fabry-Perot interferometers.
-
- P7.1: *Harang, O. and Kosch M. J.*, Absolute Optical Calibrations Using a Simple Tungsten Bulb: Theory

SESSION 1:
AURORAL PHYSICS AND
OTHER IONOSPHERIC PHENOMENA

O1.1. Optical emissions from proton aurora (Invited)

D. Lummerzheim¹ and M. Galand²

¹ University of Alaska, Geophysical Institute Fairbanks, AK 99775-7320, USA

² Boston University, Center for Space Physics Boston, MA 02215, USA

I will review modeling of proton aurora and discuss predictions of models of proton aurora. Hydrogen emissions show characteristic Doppler shifts. The hydrogen line profile depends on the energy of the precipitating protons. For ground based observations in the magnetic zenith, an elevated blue wing arises from energetic precipitation, the red wing is indicative of angular scattering. Secondary electrons in proton aurora lead to the excitation and emission of the same spectral features as seen in electron aurora. Due to the low mean energy of these secondary electrons (compared with those in electron aurora), the relative brightness of auroral emission lines and bands differs in electron and proton aurora. I will discuss these model predictions and compare ground and space based observations to these predictions.

O1.2. High-latitude artificial aurora from heating: a unique phenomenon? (Invited)

M. J. Kosch¹, M. T. Rietveld², F. Honary¹ and T. Hagfors²

¹ Communication Systems, University of Lancaster, LA1 4YR Lancaster, UK

² Max-Planck-Institut für Aeronomie, 37191 Katlenburg-Lindau, Germany

The EISCAT HF-facility (69.59 N, 19.23 E) is capable of transmitting up to 240 MW of power into the ionosphere around 4 MHz. During such O-mode transmissions soon after sunset, F-region electrons were accelerated sufficiently to excite the oxygen atoms, resulting in observable optical emissions. The O1D and O1S emissions at 630 and 557.7 nm are stimulated by electrons with energies above 1.96 and 4.17 eV threshold, respectively. It has been found that the O1D emission and electron temperature enhancements maximise near the magnetic field aligned direction regardless of the HF transmitter beam pointing direction. This is not consistent with similar lower latitude observations. The strongest optical emission and electron temperature enhancement is always produced when HF-pumping along the magnetic field line. There is also little evidence of the artificial aurora moving with either the ion convection or the neutral wind. A very faint O1S emission has been observed for the first time at high latitudes. Quenching effects suggest electrons over 6 eV are present. Frequency stepping the HF transmitter through the third gyro-harmonic results in a weakening of the optical intensity and HF coherent radar backscatter. This fact suggests that electron acceleration is closely related to the production of HF-induced upper hybrid waves. However, for lower latitudes, electron acceleration by Langmuir turbulence has been put forward as the production mechanism.

O1.3. Energy dependence of the latitude of the equatorward edge of significant proton auroral precipitation.

Eric Donovan¹, Brian Jackel¹, Robert Strangeway², and Fokke Creutzberg³

¹ University of Calgary Department of Physics and Astronomy, University of Calgary, Calgary, Canada T2N 1N4

² University of California, Los Angeles Institute of Geophysics and Planetary Physics, 2712 Slichter Hall, Box 951567 Los Angeles, California 90095-1567 USA

³ Keometrics

Proton auroral emissions are a direct result of the precipitation of Central Plasma Sheet protons. Ion distribution functions obtained from satellite passages through the auroral zone indicate that the precipitation is due to strong pitch angle scattering. With this in mind, the equatorward edge of the significant ion precipitation, and hence of the proton aurora, is the ion Isotropy Boundary (IB). The latitude of the IB depends on local time, the state of the magnetosphere, and on the energy of the precipitating ions. On the basis of simulations of proton trajectories in model magnetospheres [Sergeev and Tsyganenko, *Planet.Space Sci.*, V 30, pp. 999-1006, 1982], the observed dependence of the latitude of the IB on energy for 100-900 KeV protons [Imhoff et. al., *J. Geophys. Res.*, V 82, pp. 5215-5221], and the correlation between the IB latitude and the inclination of the magnetic field at geosynchronous orbit [Sergeev et. al., *J. Geophys. Res.*, V 98, pp. 7609-7620, 1993], it has been argued that the likely cause of the above mentioned pitch angle scattering is due to slight non-adiabatic effects due to the relatively large gyro-radii of the protons in the vicinity of the neutral sheet. We use data from roughly 1000 FAST satellite transits of the auroral oval to explore the dependence of the IB latitude on energy in the energy range ~0.5~25 KeV. Our survey of these 1000 auroral oval crossings yielded roughly 200 examples where there was a clear ordering of IB with energy. Of these, roughly half were ordered such that higher energy IBs occurred at lower latitudes, consistent with the ordering one would expect if the pitch angle scattering is due to scattering in the highly-curved field lines near the neutral sheet. On the other hand, roughly half of these were ordered with lower energy IBs equatorward of higher energy IBs. Furthermore, we find that it is more likely that an ordering consistent with the pitch angle scattering being caused by highly curved field lines occurs in the evening sector, and the opposite ordering occurring in the morning sector. These results have significant implications in the use of the equatorward boundary as an indicator of the state of the inner magnetosphere.

O1.4. Study of auroral arc fine structure with conjugate FAST and ALIS measurements

T. Sergienko¹, B. Gustavsson¹, U. Brändström¹, Å. Steen², and L. Andersson³

¹ Swedish Institute of Space Physics, P.O. Box 812, 98128 Kiruna, Sweden.

² Remspace group, Rekrytgatan 2, 58214 Linköping, Sweden.

³ Laboratory for Atmospheric and Space Physics (LASP), 1234 Innovation Drive Campus Box 590, Boulder CO 80303, USA.

Modeling the auroral optical emissions was used for quantitative study of the multi arc auroral system. High time resolution data of the auroral electron spectra measured from the FAST satellite were used as input parameters to calculate the 2D distribution of volume emission rate of the oxygen 'green line'. Calculated intensities were compared with the conjugate ALIS measurements. Results of comparison are discussed.

O1.5. Neutral winds in the e-layer of auroral zone during quiet and disturbed conditions

Sergej V. Leontyev

Polar Geophysical Institute, Apatity, 184200, Russia

Statistical study of vertical winds within auroral zone was carried out. It was demonstrated that in quiet conditions, if there are no any aurora and magnetic disturbances, the vertical wind velocity remains constant within the range 5 m/s, during the entire observation period. It allows us to use this value as a zero reference point ("rest wavelength"), corresponding to the wavelength of emission emitted by unmoving gas, when velocities of neutral wind are measured. Under disturbed conditions, vertical winds undergo considerable (up to 100 m/s) variations both at night and from night to night. Large variations of wind velocity are connected to aurora and spatial size of these disturbances is more than 200 km. During the 1998-1999 season, mean vertical winds during quiet and disturbed conditions are different. Mean vertical wind under disturbed conditions is upward relative to quiet one and its value is approximately 60 m/s. An example of vertical wind observations at two different points is given. In disturbed condition the gradient of vertical wind is very big so they may be directed in the opposite directions at distance about 100 km.

This work has been supported by the grant N 98-05-64435 from the Russian Foundation for Basic Researches.

O1.6. Multiple poleward propagating auroral events in the 15-16 MLT sector

V. Safargaleev and V. Tagirov

Polar Geophysical Institute, Apatity, 184200, Russia

We present the first results of the aurora observational campaign carried out by Polar Geophysical Institute in December 2000 - March 2001 on Spitsbergen island. Combined television, DMSP satellite and radar observations of several periodic auroral events near the polar cap boundary are reported. The events occurred within the boundary plasma sheet (bps) and presented the rayed auroral arcs appearing periodically near the bps equatorial edge, moving through the bps poleward and disappearing near its pole edge. In the DMSP spectrograms the rayed arcs were associated with the precipitating electrons with energy of 1-10 keV. It was also found that the area filled with rayed arcs (ionospheric projection of the bps) moved poleward after the northward turning of the IMF Bz and moved equatorward after Bz became negative. The time delay between the Bz turning and the aurora response is about 30 minutes and seems to depend on the sign of By. The rayed arcs moved poleward inside the bps for both positive and negative Bz. The meridian component of the convection velocity in the vicinity of the moving arc is also directed northward. The possible interpretation of the observations is suggested.

O1.7. Characteristics of the noon poleward moving auroral arcs inferred from EISCAT radar measurements.

A. Kozlovsky

University of Oulu, P.O. Box 3000, FIN-90014 Oulu, Finland

Near-noon auroral arcs were monitored by the all-sky camera on Svalbard in December 1998. Ionospheric parameters in a vicinity of the arcs were derived from the EISCAT (ESR and VHF) radar measurements. It has been found that the noon auroral arcs move poleward at the velocity of the order of 200 - 600 m/s, and this velocity does not show any dependence on the velocity of the ionospheric plasma convection along the same direction. Decrease of the background luminosity and ionospheric plasma density occurred adjacent to the arcs. Ionospheric plasma drift and ground magnetometer data show location of the auroras equatorward of the convection reversal, and particle precipitation data from DMSP satellites show their location in a vicinity of the boundary between BPS and closed LLBL. Spectrums of the northward electric field variations measured by the radar demonstrate clear peaks corresponding to the magnetic field line eigenfrequency oscillations. The observed features allow to suggest that the noon auroral arcs arise on closed magnetic field lines as a result of interference between Alfvén field line eigenmode toroidal oscillations on different L-shells.

O1.8. Ground-based optical observations of dayside aurora at Zhong Shan station in Antarctic.

V. Pitkänen¹, K. Kaila¹, Y. Yaping² and C. Chong²

¹ University of Oulu, Department of Physical Sciences

² China Research Institute of Radiowave Propagation

This paper includes at first a short review of dayside aurora. Until now most of dayside aurora observations in Antarctic have been made at South Pole station (corrected geomagnetic latitude 74,9° S).

In this research narrow field multichannel photometer measurements of aurora have been made at the Chinese Zhong Shan station (CGMLAT 74,5° S) in Antarctic. The measurements were done mainly during the Antarctic winter periods from March until September in the years 1997-1999. Photometer is recording proton H_{β} , oxygen red (630 nm) and nitrogen N_2^+ emissions also in the vicinity of local magnetic noon. First results of this research will be presented.

We suggest that these emissions are dayside auroral signatures of magnetospheric cusp/cleft. Photometer with narrow field of view gives the absolute intensities of the auroral forms and besides information about temperature in the source region of auroral emissions. Rotational temperature can be inferred from the N_2^+1 NG band.

O1.9. Auroral phenomena as seen from spacecraft auroral UV images (a review)

W. Lyatsky^{1,2}, L. L. Cogger³ and A. M. Hamza²

¹ Polar Geophysical Institute, Apatiy, Russia

² Physics Department, University of New Brunswick, N.B., Canada

³ Institute for Space Research, University of Calgary, Calgary, AB, Canada

Auroral phenomena as observed by Viking and Interball spacecrafts UV imagers have some specific features because of auroral UV imagers have relatively rough spatial (about 100 km) and temporal (usually about 1 minute) resolution, however, they allow us to see two dimensional dynamics of auroras around whole the high-latitude region. There types of auroral events are considered: auroras around the cusp/cleft region and their dependence on IMF By magnetic field, auroral phenomena in the polar cap, and auroral phenomena related to substorm generation.

Some references:

Lyatsky, W., L. L. Cogger, B. Jackel, A. M. Hamza, W. J. Hughes, D. Murr, and Ole Rasmussen, Substorm development as observed by Interball UV imager and 2-D magnetic array, *J. Atmos. Solar-Terr. Phys.*, in press 2001.

Trondsen, T. S., W. Lyatsky, L. L. Cogger, and J. S. Murphree, Interplanetary magnetic field by control of dayside auroras, *J. Atmos. Solar-Terr. Phys.*, 61, 829 - 840, 1999.

Hamza, A. M., W. Lyatsky, L. L. Cogger and J. Watermann, Geomagnetic pulsations during auroral substorms, *J. Geophys. Res.*, submitted.

O1.10. Modelling of pulsating aurora observed by EISCAT with the detailed Sodankyla ion-neutral chemistry model

Thomas Ulich¹, Esa Turunen¹, Pekka Verronen², Tuomo Nygrén³, and Francis Sedgmore-Schulthess⁴

¹ Sodankylä Geophysical Observatory, Sodankylä, Finland

² Finnish Meteorological Institute, Geophysical Research, Helsinki, Finland

³ Dept. of Physical Sciences, University of Oulu, Oulu, Finland

⁴ Danish Space Research Institute, Copenhagen, Denmark

On 17th December 1990, the UHF radar of the EISCAT Scientific Association in Tromso, Norway, was running the Finnish PULSE experiment, which has a very high temporal and spatial resolution. During the experiment, between 0245 UT and 0330 UT, a series of precipitation bursts of auroral electrons was observed by the radar. A nearby photometer, whose field of view coincided with that of the radar, observed pulsating aurora. In the present paper, we study the event by means of the revised Sodankylä Ion Chemistry (SIC) model. Recently, the model was upgraded in order to quantify the effects of particle precipitation on the neutral mesospheric chemical composition. Ionization caused by precipitating particles leads to enhanced production of some minor neutral constituents (such as NO) through reaction chains in which ionic reactions play an important role. Nitric oxides, in turn, are responsible for the destruction of mesospheric ozone. We model the temporal evolution of selected neutral and ionic species during the event between 90 and 100 km altitude by means of the time-dependent SIC model. Furthermore, we will study the temporal and spatial behaviour of the effective recombination coefficient.

O1.11. TV observations of auroral forms at different zones of high latitudes (review).

Tagirov V.R.

Polar Geophysical Institute, Russian Academy of Sciences, 184200, Apatity, Russia.

The base of report is the results of TV observations of different auroral forms made by Polar Geophysical Institute and Finnish collaborators in the auroral zone polar cap and cusp region. The auroral zone forms were pulsating aurora and torch (omega) like structures, observed by stations in Scandinavia and Kola Peninsula. Clear connection of pulsating auroral patches with ELF-VLF emissions are shown. The results of height measurements and the mapping of auroral torches to magnetospheric equatorial plane are presented. We also present the results of observations of discrete auroral rayed structures during the interaction of magnetic cloud with the Earth's magnetosphere studied for the time interval from 04.17 to 10.30 UT on 14.01.1988. TV observations were carried out in Franz-Joseph Land (Heiss Island) and covered the whole dayside sector corresponding to the event. Auroral forms represented very active rayed forms travelling mostly in azimuth direction with velocities about several kilometers per second. The polar plots of auroral motion showed the moving, which followed to "inverse" twin-cell convection pattern with sunward flow over the pole.

O1.12. Cosmic Radio Noise Absorption Associated with North-South Aurora.

M. Danielides¹, S. Shalimov², and J. Kangas³

¹ Department of Physical Sciences, P.O. Box 3000, FIN-90014 University of Oulu, Finland.

² Institute of Physics of the Earth, Moscow, Russia.

³ Sodankylä Geophysical Observatory, FIN-99600 Sodankylä, Finland.

We report first observations of cosmic radio noise absorption signature of the north-south (N-S) aurora. The N-S auroral structures are auroral forms, which originate in the wake of the westward travelling surge. We used Imaging Riometer for Ionospheric Studies (IRIS) and All-Sky Camera (ASC) data from Kilpisjärvi, Finland in order to analyse the development of both absorption and auroral distribution on October 25, 1999. Herefore a new routine was developed which allows mapping of both imaging riometer images and auroral forms into a geographic coordinate system. In this case study we found that the development of the N-S aligned auroral structures are associated with specific N-S aligned localized absorption events (only with a duration of few minutes) resembling their ASC counterparts and accompanying by Hall current jets and PiB pulsation activity.

Finally, an approach to explain the generation of the observed N-S aurora will be given and a connection to the magnetic and PiB pulsation signatures will be discussed.

O1.13. Visualization of physical processes related to combined electron-proton aurorae. software for science and education.

B.V. Kozelov¹, T. Bösinger²

¹Polar Geophysical Institute, Apatity, 184200 Russia

²University of Oulu, Oulu, Finland

The Polar Geophysical Institute of Apatity/Russia in close cooperation with the University of Oulu/Finland has developed software composed of a series of modules which can serve as a tool for quick estimates in every-day situations of auroral research. The software developing was started beginning in summer 1998 with the support of the Centre for International Mobility (CIMO, Helsinki, Finland), University of Oulu (Oulu, Finland), and Polar Geophysical Institute (Apatity, Russia). Now the main modules of the software were revised and improved and several additional modules have been developed. The BEAM module allows to examine the absorption of protons and electrons of varying energy in the Earth's atmosphere as well as in homogeneous gases. The SPUTNIK module is a simulator of simultaneous observations of precipitating particles (electrons and protons) by low-altitude satellites and by ground-based detection of the corresponding features in the ionosphere caused by these particles. The transport simulation code is based on previous works by Kozelov B.V., Sergienko T.I. and Ivanov V.E. published from 1991 to 1996. The code includes effects of multi-component atmosphere and dipolar magnetic field. Some modules contains the widely used statistical models. The MSIS-90 module, for example, is a standard model of the Earth's atmosphere used in a variety of different geophysical investigations. The HARDY module is a statistical model of particles precipitation pattern.

The software also contains the special educational modules (LECTURES, SimpleAtm), and therefore it can assist the students with understanding basic physical processes, which give rise to aurorae. While designed as an adjunct to a lecture course in auroral physics, some of these modules could be used when teaching other geophysical topics as well.

O1.14. Auroral arc and substorm generation: theory and observations (a review) (Invited)

W. Lyatsky^{1,2} and A. M. Hamza¹

¹ Physics Department, University of New Brunswick, Fredericton, N.B., Canada

² Polar Geophysical Institute, Apatity, Russia

Tight connection between auroral arcs and upward field-aligned current, surprising narrowness of the arcs as well as their fast generation allow us to consider them to be a result of a magnetosphere-ionosphere coupling feedback instability. Three types of the instability have been proposed: The Alfvén wave oscillation instability by Sato and Holzer [1973], the instability on Alfvén wings by Leontyev and Lyatsky [1982], and the ion demagnetisation instability considering ion demagnetisation in the plasma sheet to be a possible cause for field-aligned currents responsible for auroral arc generation [Kozlovsky and Lyatsky, 1999]. The physics of the latter is not trivial but simple. Because of partial ion demagnetization in the plasma sheet, electrons can drift through the relatively immobile hot ion distribution. This leads to transverse magnetospheric currents directed along convection streams, which close field-aligned currents that in turn lead to field-aligned electric field and particle acceleration needed for auroral arc generation. This instability leads to the separation of the large-scale magnetospheric convection into narrow streams, which may be responsible for auroral arc generation. The magnitude of growth rate for all the three types of the instability is estimated and expected theoretical predictions are compared with experimental data.

A theoretical basis why magnetosphere-ionosphere coupling is important for substorm generation is that ionospheric conductivity increases during substorms by 100 times. Such strong increase in the conductivity affects strongly the electric field and field-aligned current distribution and cannot be unimportant for substorm generation. However, we show that the effect of ionospheric conductivity on field-aligned current distribution and an inverse effect of field-aligned currents on conductivity variation are not only a necessary but sufficient link to provide a sudden and fast energy release that takes place during substorms, and to explain most important features of substorm development. This theory is based on a 2-D self-consistent solution for the electric field and field-aligned currents in the nightside magnetosphere-ionosphere system as a function of ionospheric conductivity. It is shown that the convection in the nightside magnetosphere is unstable and its increase leads to a strong magnetosphere-ionosphere coupling instability, which results in a fast explosion-like increase in field-aligned currents and particle acceleration. This instability requires neither reconnection nor current disruption and may appear even in quasi-dipole magnetic field configuration.

O1.15. Preliminary Results of Observations Acquired with the Hittes Spectrograph on Svalbard: The H β Line Profile, The 1NG (1,3) Band and the OII Multiplet 1(4P-4D)

D. Lummerzheim¹, M. H. Rees^{1,2}, B. S. Lanhester², S. C. Robertson², and I. Furniss³

¹Geophysical Institute, University of Alaska, USA

²University of Southampton, SO17 1BJ, UK

³University College London, W1P 7PP, UK

An unusually intense energetic proton precipitation event occurred on 26 November 2000. The resulting emission rate of Hydrogen β amounted to several hundred Rayleighs. This made it possible to examine the line profile at 1.3 Å resolution in 60 seconds exposures for several hours in magnetic zenith. We confirm the existence of a significant red-shifted component, the result of upward flowing emitting hydrogen atoms. The N₂⁺ 1NG (1,3) filter showed, in addition to the nitrogen ion band, several lines of the atomic oxygen ion of the (4P-4D) multiplet 1. This observation indicates that the incident proton spectrum must have been in the range of a few hundred eV to perhaps a few keV energy, a conjecture corroborated by near-coincident (in time and space) measurements of proton spectra from the DMSP F-12 satellite.

O1.16: Auroral sounds, Observations and Measurements

Unto K. Laine¹, Esa Turunen², Jyrki Manninen² ja Heikki Nevanlinna³

¹HUT Laboratory of Acoustics and Audio Signal Processing,

²Sodankylä Geophysical Observatory,

³Finnish Meteorological Institute

Auroral sounds have been a real mystery of science. One year ago informal research cooperation started between three Finnish university and research units with a common goal to collect and analyse data related to auroral sounds. This is a preliminary report of the first outcomes. First, the reasons why auroral sounds have been so difficult to record, even though many people have heard them, are explained by comparing the human auditory system to sound measuring and recording systems of the past and present. Over 200 reports on auroral sounds have been collected in Finland in two years. The common features of these independent reports are discussed next. Finally, some preliminary results of the analysis of auroral sound recordings are given and some new hypotheses of the possible producing mechanism of these sounds are discussed. The most interesting and rich sound material is recorded during two G4 geomagnetic storms 6.-7.4.2000 and 11.-12.4.2001. A closer analysis of these findings is still going on.

P1.1. The Red Type-A Auroras during Superstorms Caused by Coronal Mass Ejection (CMEs)

L.Yevlashin and **S.Chernouss**

Polar Geophysical Institute, 14 Fersman str, Apatity, 184200 Russia

Two geomagnetic superstorms during the maximum activity phase of solar cycle 22 were chosen for the analysis of geophysical situation: October 21-22, 1989 (min Dst = -307 nT) and March 24-25, 1991 (min Dst = -298 nT). The first event is associated with the flare X13.0/4B accompanied by a coronal mass ejection (CME). The second storm might have been produced by a CME driven interplanetary shock presumably related with X9.8/3B flare.

Optical observations at low latitudes as those by Niigata and Moshiri (Japan) on October 21, 1989 showed that red aurora appeared in the two intervals of 11.40-12.00 UT and 14.10-14.25 UT. The maximum 630.0 nm intensity was estimated to have reached more than 80 kR, whilst the maximum 557.7 nm intensity reached 20 kR. Enhancements of low energy electrons below one keV were found by DMSP-corresponding to the region of auroral intensification. On October 21, 1989 (15.00-18.00 UT) at Loparskaya obs. (Kola peninsula) red type A auroras were observed (maximum 630.0 nm intensity 25 kR, maximum 557.7 nm intensity 10 kR).

During the main phase of the storm on March 24-25, 1991 instrumental and visual observations of auroras were carried out all the night at Loparskaya observatory. The intensity ratio $I_{630.0}/I_{557.7}$ exceed 1 and red type A auroras were observed from 20.00 till 22.00 UT and also at 23.30 and 01.00 UT. It has been discovered that this auroral emission had an extremely high intensity ratio of 630.0 nm to 557.7 nm produced by low energy electron precipitation.

P1.2. Triangulation of auroral red-line emissions

Brian Jackel¹, **Eric Donovan**¹, and Fokke Creutzberg²

¹ Institute for Space Research, University of Calgary, Canada

² Keometrics, Canada

Heights of auroral emission may vary significantly, depending on the characteristics of precipitating electrons and protons. Auroral images are often projected onto geographic maps using an assumed emission height. It is therefore important to establish what range of heights typically occurs. As well, some information about incident particle energy may be inferred from knowledge of emission heights. Two meridian scanning photometers from the CANOPUS network have been used to estimate peak auroral emission heights by triangulation. In this study we concentrate on red-line (6300A) emissions, which generally occur at higher altitudes (150-300 km) and thus are better suited for joint observations from distant sites. A comparison is made between triangulation heights and a spectroscopic ratio (6300A / 4709A) commonly used for inferring characteristic energy of precipitation.

P1.3. Auroral pulsations in diffuse luminosity during substorm.

T.A. Kornilova¹, I.A. Kornilov¹, M.I. Pudovkin², O.I. Kornilov², J. Kultima³

¹ Polar Geophysical Institute, Apatity, Murmansk region, 184200, Russia.

² Institute of Physics, St.Petersburg State University, St.Petersburg, Petrodvorets, 198904, Russia.

³ Sodankyla Geophysical Observatory, FIN-996000 Sodankyla, Finland.

The behaviour of diffuse luminosity equatorward of southern boundary of the discrete auroral forms during the growth phase of substorm has been investigated on the TV auroral data. The method of TV images filtering was used. Three types of auroral pulsations inside diffuse luminosity have been observed: (A)– arc-like filaments inside diffuse luminosity pulsating with the period of ~ 3-10 s, (B) – auroral pulsations of the southern boundary of diffuse luminosity with the period ~ 30-40 s, (C)–auroral arc-like structures pulsating with the period of 30-50 s appearing with the period of 30-70 s on the south boundary of localised “resonator” region and spreading northward with the velocity of ~0.2-0.8 km/s simultaneously with the same structures appearing on the north boundary and spreading southward. In the course of growth phase one or two types of pulsations may be observed in diffuse luminosity at the same time. All three types of aurora pulsations are conducted by geomagnetic ones of the same periods. Wavelet analysis has been used to reveal fine details of spectrum-time structure of geomagnetic pulsations. The substorm expansive phase represented by extension of bright diffuse region having internal structure as patches and arc fragments is more often preceded by the auroral pulsations of (A) type. (B) and (C) types precede the explosive phase when poleward expansion is looking like arc jumps into more polar latitudes. Different pulsation types and their localisation inside diffuse luminosity can be a result of plasma gradients existence (density, temperature, energy and so on) and display the interaction of different magnetosphere regions and so can give important information about magnetosphere structure.

P1.4. Auroral Structures and Emissions in the Antarctic

Kari Kaila¹, Veli Pitkänen¹, Hannu Holma¹, Jouni Jussila¹, Yuan Yaping² and Cao Chong²

¹ University of Oulu, Department of Physical Sciences

² China Research Institute of Radiowave Propagation

A Finnish multichannel auroral photometer has been in operation in Chinese Antarctic station Zhong Shan (69.37° S, 76.37° E, CGM 74,5° S). The station is located in the polar cup region, where the night time aurora is rarely seen. The daytime aurora can be observed close to the noon around midsummer. The local noon is close to 10.30 UT and the earliest measurements have been started at 11 UT.

The nighttime aurorae will sometimes spread to high latitudes. The typical auroral oval at night time is far equator ward from the station. During substorms the most poleward aurorae can reach the station. Pulsating aurora are occasionally observed.

The auroral photometer made at the university of Oulu had five channels during 1997-1999 and six channels since 2001. They measure auroral emission with three different modes. The photometer tubes have a field of view of 2° except in H_β, which has a field of view of 3°. Due to the rare nighttime aurora most of the photometer measurements are not aurora, but only airglow.

During the darkest months, in June and early July, it is possible to measure daytime aurora due to the geometry of the oval. The big difference of the directions of the magnetic and geographical poles permits the very early afternoon observations of aurorae. The prenoon observations under dark sky are impossible.

P1.5. Electron energy estimations in an auroral arc

H. Holma, K. Kaila and J. Jussila

Department of Physical Sciences, P.O.Box 3000, FIN-90014 University of Oulu, Finland

An arc-like auroral form passed twice over the magnetic zenith at Kilpisjärvi (68.47N, 22.44E), Finland, on 31st January 2001. The form was measured by a zenith-photometer at Kilpisjärvi and by a scanning photometer at Karesuvanto about 150 km Southeast from Kilpisjärvi. The form is studied in terms of rotational temperature in order to estimate energies of precipitating particles causing the emissions. The zenith-photometer is used to clarify the total flux of the electrons and effective emission height, whereas the scanning photometer gives the intensity distribution over the height.

SESSION 2:
AURORAL OBSERVATIONS
MONITORING MAGNETOSPHERIC PHENOMENA
AND SPACE BORN STUDIES

O2.1. Electrodynamics of auroral arcs (Invited)

A. T. Aikio

Department of Physical Sciences, University of Oulu, P.O. Box 3000, FIN-90014
University of Oulu, FINLAND

A short review of the electrodynamic of stable auroral arcs will be given. Observations of electric fields, horizontal and field-aligned currents in the vicinity of arcs will be shown. Also, satellite observations of the auroral acceleration region will be presented. Finally, the linear current-voltage relationship will be discussed.

O2.2. Auroral signatures of dayside boundary layer dynamics. (Invited)

J. Moen^{1,2}

¹ Department of Physics, University of Oslo, P.o. Box 1048 Blindern, N-0316 Oslo,
Norway

² Also at Arctic Geophysics, University Courses on Svalbard, N-9170 Longyearbyen,
Norway

The cusp configuration and the polar cap convection are known to be regulated by the orientation of the interplanetary magnetic field (IMF). The IMF B_Y control of the cusp position is a unique signature of magnetic reconnection. The IMF B_Y control of the motion pattern and the location of cusp auroral activity was for the first time continuously monitored in a case when IMF B_Y went from -15 nT to +15 nT. The zonal shift in the cusp position was estimated to be at least three hours in magnetic local time, and the cusp reconfigured within a few minutes after B_Y changed polarity at the magnetopause. On January 14, 2001 Cluster encountered a similar transient reconfiguration of the cusp. The cusp expanded over the spacecraft into the late postnoon sector. NOAA-12 probed the 1630 MLT sector of corresponding auroral activity, and measured a 1.4 keV electron beam located poleward of the 30 keV electron-trapping boundary. A prominent example of discrete postnoon aurora on open field lines, which is thought of as unusual. Sometimes the cusp is spatially bifurcated relative to its source regions. An example will be shown demonstrating that auroral signatures of Northern and Southern Hemisphere reconnection may be observed within the same all-sky image. The need for multi-site observations of auroral phenomena will be emphasised.

O2.3. Analysis of auroral signatures and electrodynamics of a pseudobreakup event, using observations of the MIRACLE network

O. Amm¹, P. Janhunen¹, K. Kauristie¹, H.J. Opgenoorth^{1,2}, T.I. Pulkkinen¹, and A. Viljanen¹

¹ FMI, Geophysical Research, Vuorikatu 15 A, FIN - 00101 Helsinki, Finland

² Swedish Institute of Space Physics, Uppsala Division Ångström Laboratory, Lägerhyddsvägen 1, S-75591 Uppsala, Sweden

A short-lived auroral spiral is observed on February 3, 1999, around 2204 UT, using the MIRACLE network of ground-based instruments in Fennoscandia which consists of magnetometers, coherent scatter radars, and all-sky cameras. Four minutes later, after this spiral has subsided, the auroral bulge of a fully developed substorm that has set on earlier over Russia, intrudes into the MIRACLE field of view from the east. Hence, the auroral spiral precedes the substorm spatially (i.e., it is located westward of the substorm bulge) rather than temporarily. Since this spiral is associated with a localised and short-lived substorm-type auroral development, we interpret it as a "pseudobreakup spiral", which is subsequently covered by the intruding auroral bulge, during the decaying phase of the pseudobreakup activity. In contrast to growth phase pseudobreakups that occur temporally before a full breakup, this pseudobreakup is observed spatially ahead (westward) of an already evolving substorm bulge. Our instantaneous spatial analysis of the distributions of ionospheric electrodynamic parameters associated with this spiral shows that all key features are similar to the ionospheric electrodynamics of the westward traveling surge (WTS): A sharp decrease of conductance towards the west, from Hall conductance values up to 30 S in the spiral to less than 2 S west of it, a cluster of upward field-aligned currents (FAC) in the spiral area with magnitudes up to 5 A/km², and anticlockwise spiraling horizontal currents around it. The upward FACs, diverging at least 100 kA of current in total, are fed to a large extent by a "pseudo-substorm electrojet" carried by westward flowing Hall currents. No signs of local current closure by downward FACs from the immediate vicinity of the spiral are found. Our results are inconsistent with the earlier conjecture that insufficient ionospheric conductance would prevent the pseudobreakup to evolve to a full breakup. Since the solar wind data does not provide clear evidence for being a driver of the pseudobreakup-breakup sequence, the driver has to be an internal magnetospheric one.

O2.4. Monitoring the Ion Isotropy Boundary with Multipoint Proton Auroral Measurements

N. A. Nicholson¹, E. F. Donovan¹, B. J. Jackel¹, L. L. Cogger¹, T. Sotirelis², I. Voronkov³, F. Creutzberg⁴

¹Department of Physics and Astronomy, University of Calgary, 2500 University Drive N.W. Calgary, Alberta, Canada T2N 1N4

² Johns Hopkins Applied Physics Laboratory, 11000 Johns Hopkins Road, Laurel, Maryland, USA 20723-6099

³ Department of Physics, University of Alberta, 412 Avadh Bhatia Physics laboratory, Edmonton, Alberta, Canada T6G 2J1

⁴ Keometrics, c/o Room 2037 - 100 Sussex Drive, Ottawa, Ontario, Canada K1A 0R6

A Meridian Scanning Photometer (MSP) has been operated at Gillam, Manitoba ($\lambda = 4$) over the last decade. This instrument routinely obtains meridional scans of auroral emissions at a number of wavelengths, including the 4861 Å hydrogen Balmer "beta" line. We have identified times when the proton auroral data is not compromised by cloud, moonlight or twilight. In all, we have roughly 300,000 meridional scans obtained between 1990 and 1999. We compare intensities from ~50 meridional scans with ion precipitation data from DMSP overflights. In so doing, we demonstrate that we can identify the ion isotropy (or IB) boundary by locating the equatorward edge of the diffuse H β -emissions. On this basis, we assert that the ~300,000 meridional scans provide roughly that many estimates of the latitude of the isotropy boundary. We show that the statistical behaviour of proton auroral IB estimates is consistent with that of NOAA spacecraft based estimates as described in {Sergeev and Gvozdevsky} [Ann. Geophys., 13, 1093-1103, 1995]. In order to explore the coherency of this boundary as a function of local time, we compare near-simultaneous IB observations obtained at different local times from several platforms. We will be focussing on multipoint measurements of this boundary and examining how they compare to an empirical model.

O2.5. Using image filtering methods for TV data processing: Subvisual auroral wave structures and pulsations

I.A. Kornilov¹, T.A. Kornilova¹, O.I. Kornilov²

¹ Polar Geophysical Institute, Murmansk region, Apatity, 184200, Russia

² Institute of Physics, St. Petersburg State University, St. Petersburg, Petrodvorets, 198904, Russia.

Short description of some image processing methods is presented with a main attention to the methods of image filtering (gradient, convolution, FFT, AR-models, SVD and others). Examples of using these methods for TV data processing (frames and keograms) demonstrate surprising improvement of experimental material. Many invisible in the initial data fine details can be revealed and some disturbing TV observations factors (fog, clouds, twilight, city lights, etc) are strongly suppressed. Filtering allowed to study some fine details in a previously known geophysical phenomena and find some principally new:

1. Fast pulsations south from the arc, moving southward before the breakup. Period of pulsations is about 3-10 s.

2. High speed spreadings and motions of pulsating patches at the time scale about 100-200 ms and detection of a small changers in pulsating aurora at the neighbor TV fields (scale 20 ms). Effect corresponds to the fine VLF chorus structure.

3. Waves of luminosity, generated by auroral activity and moving north and south with a speed 0.1-0.3 km/s and periods 1-2 min. Waves can be seen in the different regions of auroral oval from Lovozero to Svalbard.

4. Breakup precursors, appearing above Svalbard as a very weak subvisual narrow arcs 10-30 minutes before breakup in the auroral zone. Arcs moving north with a speed about 0.2-0.4 km/s.

4. Subvisual pulsations at the southern border of diffuse luminosity with a period 30-40 s. There is a tendency for pulsations to anticorrelate with the main auroral activity at the North and Zenith.

5. Waves and pulsations, moving North and South inside diffuse luminosity band with a size about 100-200 km in N-S direction. Probably, the waves were captured in a resonator, formed by plasma gradients at the northern and southern borders of diffuse luminosity.

Image processing procedures can be also used for the enhancement and improvement of any other information, presented as a 2-dimensional picture (scanning photometers data, VLF and magnetic pulsations frequency spectra and so on).

O2.6. HF radar observations of auroral boundaries

G. Starkov¹, P. Eglitis^{2,3}, M. Uspensky^{2,4}, A. Fabirovsky⁴, B. Kozelov¹, K. Kauristie²,

¹ Polar Geophysical Institute, Apatity, 184200 Murmansk region

² Finnish Meteorological Institute, Vuorikatu 15A, FIN-00101 Helsinki

³ Swedish Institute of Space Physics, Uppsala

⁴ Murmansk State Technical University, 183010 Murmansk

The Finland CUTLASS HF radar looking approximately normal to the L-shells can effectively monitor the most equatorward auroral boundary during quiet or even moderate geomagnetic conditions. This afternoon-evening sector boundary is the subvisual equatorward edge of the diffuse luminosity belt which corresponds to the magnetospheric inner edge of the electron plasma sheet. The boundary can be monitored with CUTLASS because of its relatively low magnetic latitude and nearly-zero off-orthogonal angles which enable the radar to collect the E-layer echoes. The echo signature is a narrow in range (1-3 range gates) and persistent band of the auroral F- and E-layer echoes which gradually moves equatorward, consistent with the luminosity belt diurnal rotation.

Two other auroral boundaries, i.e. the equatorward and poleward edges of the auroral oval, can be observed by the HF radars in suitable conditions. We will present and discuss two such examples where the Iceland West and Iceland East HF radars looking also nearly normal to the L-shells observed the afternoon-evening auroral oval as a 'hole in the auroral backscatter. From the basis of DMSP particle data we can conclude that the morphological difference in the E-layer ionisation was the most probable cause for the the backscatter hole.

O2.7. Ground-based and satellite observations of high-latitude auroral activity in the dusk sector of the auroral oval.

K. Kauristie¹, T. I. Pulkkinen¹, O. Amm¹, A. Viljanen¹, M. Syrjäso¹, P. Janhunen¹, S. Massetti², S. Orsini², M. Candidi², J. Watermann³, E. Donovan⁴, P. Prikryl⁵, P. Eglitis⁶, C. Smith⁷, W. F. Denig⁸, I. Mann⁹, H. J. Opgenoorth^{1,6}, M. Lockwood¹⁰, M. Dunlop¹¹, A. Vaivads⁶, M. Andre⁶

¹ FMI/GEO, Finland, ² IFSI-CNR, Italy, ³ DMI/Solar-Terrestrial Physics Division, Denmark, ⁴ University of Calgary, Canada, ⁵ Communications Research Center, Canada, ⁶ IRF/Uppsala Division, Sweden, ⁷ Bartol Research Institute, USA, ⁸ Air Force Research Laboratory, USA, ⁹ University of York, UK, ¹⁰ RAL, UK, ¹¹ Imperial college, UK

On Dec 07 2000, during 1330-1530 UT the MIRACLE all-sky camera at Ny Ålesund observed auroras at high latitudes (MLAT~76) simultaneously when the Cluster spacecraft were skimming the magnetopause in the same MLT sector (at 16-18 MLT). The location of the auroras (at the ionospheric convection reversal boundary) and the clear correlation between their dynamics and IMF variations suggests their close relationship with R1 currents. Consequently we can assume that the Cluster spacecraft were making observations in the magnetospheric region associated with the auroras, although exact magnetic conjugacy between the ground-based and satellite observations did not exist. The IMF Bz direction appeared to control both the behaviour of auroras and magnetopause dynamics. During periods of IMF Bz mainly negative the auroras brightened and the Cluster spacecraft experienced periodic (T 4-6 min) encounters between magnetospheric and magnetosheath plasmas. These undulations of the boundary can be interpreted to be a consequence of magnetopause surface waves. Comparison of the magnetic field observations of the four spacecraft reveals that the waves were propagating tailwards, but the estimates of their phase velocities have a large scatter (mean 215 km/s, standard deviation sigma 90 km/s). When IMF Bz stayed positive for a longer period the auroras faded and the spacecraft stayed at the outer edge of the magnetopause where they observed electromagnetic pulsations (T ~ 1 min) with average tailward phase velocities of 126 km/s (sigma=26 km/s). We find these observations interesting especially from the viewpoint of previously presented studies relating high-latitude auroras with MHD waves propagating at the magnetospheric boundary layers.

P2.1.Fine details of space and time structure of pulsating aurora and VLF-chorus emissions

I.A. Kornilov

Polar Geophysical Institute, Murmansk region, Apatity, 184200, Russia

It is wellknown that ground-based VLF-chorus observations demonstrate fine chorus structure at the time scales of some milliseconds. That fact was always explained as a purely propagation effect due to the motion of chorus wave front from the region of generation through inhomogeneous magnetosphere plasma, multiple reflections in ionosphere and, consequently, summarizing in receiving VLF antenna signals with neighbor frequencies and random phases. There were no doubts, that at magnetosphere equator, in the region of generation, chorus emissions are almost clear sine signals with increasing frequency.

Using methods of autoregression (AR) models spectral analyses, providing sufficiently higher time and spectral resolution than ordinary FFT, it was found that both ground-based and satellite VLF-chorus emissions have fine time and spectral structure at the scale of 5-20 Hz and 10-20 milliseconds correspondingly. So fine chorus structure is not a propagation effect, chorus are structured initially, in the region of generation and this is a result of unknown details of the chorus generation mechanism. Chorus generation looks like a "chain reaction" of short individual activations. To find any manifestations of fine chorus structure in a pulsating aurora, we have investigated thousand hours of TV observations with synchronously recorded chorus and found several cases of definitely isolated pulsating patches and corresponding VLF-chorus emissions and so can say that namely this chorus was generated in that pulsating patch.

Using different TV image enhancement procedures and methods of integral projection functions it was found that good correlation between fine structure of chorus and small fast details of optical pulsations really exists. Our conclusion is that fine time, spectral and space structure of chorus and auroral pulsations is a result of close and fast interactions of the different areas of a highly structured region of generation at the magnetosphere equator.

P2.2. Using image filtering methods for TV data processing: Subvisual auroral wave structures and pulsations

T.A. Kornilova¹, I.A. Kornilov¹, M.I. Pudovkin², O.I. Kornilov², J. Kultima³

¹ Polar Geophysical Institute, Murmansk region, Apatity, 184200, Russia

² Institute of Physics, St. Petersburg State University, St. Petersburg, Petrodvorets, 198904, Russia.

³ Sodankylä Geophysical Observatory, FIN-99600, Sodankylä, Finland

The behaviour of diffuse luminosity equatorward of southern boundary of the discrete auroral forms during the growth and expansive phases of substorm has been investigated on the TV auroral data. The method of TV images filtering was used. Three types of auroral pulsations inside diffuse luminosity have been observed: (A) - arc-like filaments inside diffuse luminosity pulsating with the period of ~ 3-10s, (B) - auroral pulsations of the southern boundary of diffuse luminosity with the period ~ 30-40 s, (C) - auroral arc-like structures pulsating with the period of 30-50 s appearing with the period of 30-70 s on the south boundary of localised "resonator" region and spreading northward with the velocity of ~0.2-0.8 km/s simultaneously with the same structures appearing on the north boundary and spreading southward. In the course of growth phase one or two types of pulsations may be observed in diffuse luminosity at the same time. All three types of aurora pulsations are conducted by geomagnetic ones of the same periods. Wavelet analysis has been used to reveal fine details of spectrum-time structure of geomagnetic pulsations. The substorm expansive phase represented by extension of bright diffuse region having internal structure as patches and arc fragments is more often preceded by the auroral pulsations of (A) type. (B) and (C) types precede the explosive phase when poleward expansion is looking like arc jumps into more polar latitudes. Different pulsation types and their localisation inside diffuse luminosity can be a result of plasma gradients existence (density, temperature, energy and so on) and display the interaction of different magnetosphere regions and so can give important information about magnetosphere structure.

P2.3. All-Sky Imaging Within the Canadian CANOPUS and NORSTAR Projects

Eric Donovan, Trond Trondsen, Leroy Cogger and Brian Jackel

Department of Physics and Astronomy, University of Calgary, Calgary T2N 1N4, Canada

In 1986, a digital All-Sky Imager (ASI) was deployed in Gillam, Canada, as part of the CANOPUS ground-based observational program. The CANOPUS ASI operated during winter months over the next fifteen years, and was finally removed from the Gillam site in April of 2001. In the fall of 2000, three new ASIs were deployed in Gillam, Rankin Inlet, and Resolute Bay. These imagers were deployed and operated as part of the combined CANOPUS-NORSTAR program. We expect to continue operating these three imagers, and to augment this array with two to three more ASIs, over the next several years.

We discuss the technical specifications (including calibration, optics, field of view, and sensitivity) of the original CANOPUS ASI, as well as the newer CANOPUS/NORSTAR imagers. We review scientific accomplishments of the CANOPUS ASI program, and discuss ongoing research work involving the original data set. Finally, we present highlights of data from the new imager array, and discuss the scientific goals of the expanded CANOPUS/NORSTAR ASI program.

P2.4. Developing of auroral intensification as an output of magnetosphere-ionosphere dynamical system

B.V. Kozelov and T.V. Kozelova

Polar Geophysical Institute, Apatity, 184200 Russia

Using TV data observations we analyse the developing of different kinds of auroral intensifications. The set of TV images is considered as an output of magnetosphere-ionosphere dynamical system. To characterise the complicity of the auroral image we use the fractal dimension spectrum of lines of equal intensity. By the spectrum we can localize the auroral form from background noise and can select the most variable intensity level. The modification of Grassberger-Procacci method has been used for searching of the low-dimensional dynamics of the magnetosphere-ionosphere system, which generates the image set. This our consideration is mainly aimed on difference between pseudo-breakups and major substorm onsets.

P2.5. Azimuthal Propagation of the Auroral Arcs

V. Safargaleev, S. Osipenko and V. Tagirov

Polar Geophysical Institute, 184200, Apatity, Russia

Abstract: Auroral arc dynamic was investigated using of the high-resolution TV registration of auroras in Barentsburg (14.12 E; 78.05 N) in combination with HANK radar data. We concentrated on the events when it was possible to trace the development of the auroral arc along the azimuth. For the events in the premidnight sector it was shown that the arc appeared in the East and then expanded through the TV-camera field of view westward at the velocity of about ~5 km/s at the ionosphere altitude. It was found for the most cases, that the convection in the arc vicinity flowed in the same direction. In a few cases when the POLAR data were available, the appearance of the arc in the TV camera field of view was associated with the development of aurora bulge on the UVI images east of the observatory, so the arc seemed to be originated from that area. This result is important for understanding the nature of the auroral arc. The possible mechanism of arc formation is discussed in terms of the convection instability.

P2.6. Auroral breakup as observed from above and below: multi-instrument case study

A.G. Yahnin¹, I.A. Kornilov¹, T.A. Kornilova¹, S.V. Leontyev¹, L.A. Frank², J.B. Sigwarth², K. Liou³, C.-I. Meng³, T. Mukai⁴, S. Kokubun⁵

¹ Polar Geophysical Institute, Apatity, Murmansk region, Russia

² Department of Physics and Astronomy, University of Iowa, Iowa City, USA

³ Applied Physics Laboratory, Johns Hopkins University, Laurel, Maryland, USA

⁴ The Institute of Space and Astronautical Science, Sagami-hara, Kanagawa, Japan

⁵ Solar-Terrestrial Environment Laboratory, Nagoya University, Toyokawa, Japan

We performed a study of phenomena around the substorm onset with emphasis on fine details of the auroral arc brightening. The breakup occurred at around 1923 UT on 8 February 1997 above the observatory Lovozero where the all-sky auroral TV camera and multi-channel photometer were in operation. Joint analysis of the ground TV camera data and the Polar UV and VIS images enable us to determine the location and size of the onset region. We found that the initial brightening of the auroral arc appeared eastward of ground station in very localized (some 5 degrees of longitude) region. This suggests the magnetospheric source size of the order of 1 RE. The auroral arc, on which the breakup started, was formed as a result of splitting of the diffuse aurora several minutes before the breakup. A westward (outward from the breakup source region) movement of luminosity irregularities along the arc with the velocity of 10-15 km/s was revealed using methods of the digital filtering of auroral images. During breakup the irregularities passed through the ground-based camera field of view with a period of 15-20 s. So fast, but solitary irregularities were detected since the time of the pre-breakup arc formation, several minutes before the breakup. This may mean that instability impulsively developed in the source region both before and during the breakup, but with different repetition rate. The initial stage of the auroral breakup was not associated with any significant ground magnetic effect, so this stage might be classified as pseudobreakup. Ratio of main auroral emissions measured both from the ground and space suggests rather hard spectra of precipitating electrons, so one can expect high conductance of the ionosphere within the breakup region. We concluded that in this case the faintness of the magnetic disturbances might be due to a very small electric field in the ionosphere as well as localized nature of the current system. The Geotail spacecraft was situated in the mid-tail plasma sheet close to the meridian of auroral breakup. The spacecraft detected first perturbations in the plasma sheet and magnetic field parameters several minutes after the auroral breakup. The perturbations include the tailward plasma flow, which is a typical mid-tail signature of the substorm onset. The delay agrees with propagation of the disturbance from the near-Earth region.

P2.7. Ionospheric heating at Tromsø – Source for active space experiments

Antti J. Oikarinen

Department of Physical Sciences, PO Box 3000, FIN-90014 University of Oulu, Finland.

Ionospheric heating is done by powerful HF radio transmission. It has many applications to produce different artificial phenomena in space. In this paper heating method, equipment and some experiments are described.

SESSION 3:
ODIN; THE FIRST RESULTS

O3.1. The Odin Aeronomy Mission

Donal Murtaugh

Chalmers University of Technology, Department of Space and Radio Science,
SE- 412 961, Göteborg, Sweden

The Odin satellite was launched on 20 Feb 2001 and has begun its joint Astrophysics and Aeronomy mission. Odin is a joint project between Sweden, Finland, France and Canada with various parts of the satellite and its instruments being built in the various countries. The aeronomy mission is aimed at understanding the physical and chemical processes that control the distribution and temporal behaviour of various trace gases in the stratosphere and mesosphere, in particular ozone and water vapour as well as gases controlling the destruction of ozone.

To this end Odin carries two instruments: a sub-mm radiometer SMR and an Optical Spectrograph and Infra Red Imaging system both particularly suited to the measurement of different gases. The sub-mm region is perhaps the best region to measure ClO that is closely related to catalytic ozone destruction during the polar winters while the optical spectrograph will allow us to retrieve NO₂ as well as BrO with good precision. Both of these gases are also intimately related to the control of ozone concentrations in the stratosphere. Further because of the close cooperation with the astronomical community the SMR measures the strongest sub-mm line of water vapour making Odin especially suited for measurements in the upper mesosphere where it will be able to make single profile measurements to altitudes above 90 km.

O3.2. First Results from the OSIRIS Instrument on-board Odin

Edward J. Llewellyn

Institute of Space and Atmospheric Studies, University of Saskatchewan, 116 Science
Place, Saskatoon, SK, S7N 5E2, Canada

The OSIRIS instrument onboard Odin is a combined optical spectrograph and infrared imager that is obtaining atmospheric images when Odin is set to scan the terrestrial limb. Following a perfect launch and a three-week outgas period OSIRIS was switched on with Odin in an inertially fixed pointing mode. Thus for half of each orbit OSIRIS looked into deep space and then rapidly scanned through the atmospheric limb before observing the atmosphere in the nadir. In this last case the collected data were similar to those obtained with GOME. These first images showed that OSIRIS was meeting its design goal and that it would provide important new aeronomy data, both from the Rayleigh scattered sunlight and the airglow. These initial images also showed the oxygen A-band in emission at high tangent altitude and in absorption at low altitude.

The pointing co-alignment of the Radiometer and OSIRIS was confirmed through observations of Jupiter in which planetary full-disk spectra were obtained. In mid-May the Aeronomy commissioning phase began and Odin was put into both a limb stare mode and a limb-scanning mode. These observations showed the expected decrease in absorption with altitude and displayed a close agreement when overlaid with the pre-flight calculated spectra. A preliminary analysis of the slant ozone column data has been attempted using the Chappuis absorption feature. The infrared imager data have been used with the tomographic inversion procedure and show the existence of structures in the distribution of the airglow emission that have not been previously observed.

In this paper the early results from the initial analysis of these OSIRIS observations will be presented in some detail and the potential for other findings discussed. The opportunities for future collaborative studies of OSIRIS with the Odin Radiometer and ground-based observatories will also be described.

O3.3. The potential for incorrect interpretation of atmospheric images as seen with OSIRIS

D.A. Degenstein, E.J. Llewellyn and N. D. Lloyd

University of Saskatchewan, 116 Science Place, Saskatoon, Saskatchewan, Canada

Tomography is the representation of a three dimensional object by its two dimensional cross sections. The tomographic concept uses line integral measurements of a two dimensional field to retrieve that field. The Odin satellite was launched on February 20, 2001 and is now operational, it includes an Optical Spectrograph and InfraRed Imaging System (OSIRIS). During each orbit OSIRIS makes hundreds of thousands of line integral measurements of the atmospheric volume emission rate profiles around 1.27 and 1.53 microns. These measurements sample the atmosphere within the two dimensional satellite orbit plane and are ideal for interpretation with a tomographic technique. The developed technique uses the line of sight integrated volume emission measurements and a modified Maximum Likelihood Expectation Maximization (MLEM) algorithm to retrieve two-dimensional structure in the atmospheric volume emission profile.

In this paper the utility of the developed tomographic technique is demonstrated with examples from the OSIRIS data set. In particular it is shown that the correct interpretation of the two-dimensional volume emission rate profiles can be obtained with the use of limb imaged data and the two-dimensional tomographic analysis. It is also shown that the simple one-dimensional analysis of single limb scans may lead to errors. Finally, the capabilities of the OSIRIS measurements are discussed with respect to their usefulness for determining small and large scale horizontal structures in the Oxygen InfraRed Atmospheric and the OH Meinel band emissions.

O3.4. Early results from the Sub-MM Radiometer onboard Odin

Donal Murtaugh

Chalmers University of Technology, Department of Space and Radio Science,
SE- 412 961, Göteborg, Sweden

The sub -mm instrument on board Odin consists of 4 sub-mm receivers and one mm receiver sharing access to three spectrometers and one filterbank. The Filterbank is permanently connected to the 119 GHz receiver to monitor molecular oxygen as a method of retrieving the temperature profiles. As each of the sub-mm receivers is tunable over a wide range, we have selected to operate in a number of mode that allow us to measure the most important gases in the atmosphere.

Most of these modes have now been tested and appear to be yielding spectra similar to expectations. Even at this early stage in the data analysis it is possible to see the effects of changes in the atmospheric state in the more or less raw data. First attempts to invert the data into atmospheric profiles will be being made at about the time of this presentation.

SESSION 4:
TROPOSPHERIC AND STRATOSPHERIC
PHYSICS

O4.1. Atmospheric Research on Envisat (invited)

Gilbert W. Leppelmeier

G & S Associates

Very soon this year, ESA will launch its environmental research and monitoring satellite, Envisat, the largest and most complex mission yet taken on by ESA. Onboard will be three complementary atmospheric instruments: GOMOS, MIPAS, and SCIAMACHY. Working on very different methods, together these three instruments will provide not just monitoring of ozone, but will enable scientists to study in detail the atmospheric processes involved in ozone dynamics, climate change (read "global warming"), and atmospheric pollution from a variety of sources. Such knowledge is essential to the modeling efforts necessary for predicting the future state of the atmosphere and evaluating the consequences of various counter-measures.

O4.2. Detecting polar stratospheric clouds using the zenith-sky colour index

Carl-Fredrik Enell¹, Kerstin Stebel¹, Thomas Wagner², Klaus Pfeilsticker² and Ulrich Platt²

¹ Institutet för or yrmdfysik, Box 812, SE-98128 Kiruna

² Institut für Umweltphysik, Universität at Heidelberg, Im Neuenheimer Feld 229, D-69120 Heidelberg

Polar stratospheric clouds (PSC) develop in the cold winter polar vortex, in the Arctic especially as a result of local cooling by mountain-induced waves. Since both the large-scale temperature fields and the local wave activity have a large interannual variability this is also true for PSC presence because of the strong temperature dependence of the condensation and nucleation processes.

Since reactions on PSC particle surfaces are of major importance in the chemistry of the winter polar stratosphere, it is important to quantify the presence of PSCs. The twilight zenith-sky colour index is useful for obtaining statistics on PSC presence since it allows, properly defined, to detect PSC presence during sunrise and sunset even when Tropospheric clouds prevent direct observations. The purpose of this talk is to outline the possibilities and limitations of the method and to discuss suitable definitions of the colour index.

O4.3. The role of swapping mechanisms of atmospheric reservoir species in active chlorine accumulation in the polar stratosphere

Yu.E. Belikov, K.B. Moeseyenko

Fedorov Institute of Applied Geophysics, Rostokinskaya, 9, 129128, Moscow, Russia

There exists some regularity in the processes of accumulation and destruction of the reservoir species in the polar earth stratosphere. At transition from the polar autumn to polar winter as the solar zenith angle increases and UV radiation decreases there takes place the accumulation of those atmospheric reservoir species which can exist under these specific conditions and have long lifetime against photo dissociation processes. Vice versa, at transition from polar winter to polar summer the less stable species are destroyed first and partially converted to more stable ones. Such "swapping" processes can lead to active chlorine accumulation and odd nitrogen decrease. One of these processes has been considered in [1]. The ClONO₂ destroying can lead to accumulation of the more stable N₂O₅ and chlorine oxide ClO. The "swapping" mechanism is expressed as the set of chemical reactions: ClONO₂+hn=Cl+NO₃, Cl+O₃=ClO+O₂, NO₃+NO₂=N₂O₅

This chain leads to NO₂ molecule disappearance and ClO molecule release. Some other possible swapping mechanisms leading to ClO and BrO release are discussed.

In this paper the numerical modeling and analytical investigation of the swapping processes are described. The calculations of atmospheric solar spectrum were performed on the basis of numerical solution of the integral equation of radiative transfer. The box photochemical model accounting for the all basic gas-phase chemical reactions in the atmosphere was used for the analysis of altitudinal, latitudinal and temporal dependences of the swapping effects. It was obtained that: 1) the processes of active chlorine accumulation due to the swapping mechanisms can have "resonance" character 2) if their acting are close to resonance, the total active chlorine increase for the whole polar winter and spring approaches to that one due to the heterogeneous reactions in polar stratospheric clouds 3) the basic conditions which the swapping mechanisms depend on are: the temperature, the initial (nocturnal) concentrations of the reservoir species, the existence of the polar stratospheric clouds and their altitude and optical thickness, the vertical ozone distribution 4) the active chlorine accumulation is maximal on the poles and decreases to the middle latitudes, which is conditioned by more long and gradual reservoir destroying on the poles 5) during the polar winter and spring the active chlorine increase occurs "top-down" from the altitudes of 25-30 km to 15-20 km, which is conditioned mainly by the analogue altitude change of stratospheric temperature minimum and more intense radiation penetration to the lower stratosphere when the solar zenith angle decreases 6) the role of polar stratospheric clouds seems as follows. First is the intensification of the active chlorine increase and odd nitrogen decrease above the clouds in the regions of their shadow when the Sun is under visible horizon. Second is the strong odd nitrogen decrease under the clouds when the Sun is above horizon. The degree of odd nitrogen decrease increases exponentially depending on the optical depth of the cloud in the solar direction. Besides, the clouds preserve the reservoirs from their destruction by the direct solar flux and facilitate the more long active chlorine existence in the polar stratosphere.

1. Belikov Yu.E., Moeseyenko K.B. Influence of solar radiation attenuation by aerosol on the ozone content in the polar stratosphere, Proceedings of the QUADRENNIAL OZONE SYMPOSIUM, Hokkaido University, Sapporo, Japan 3-8 July 2000

O4.4. NOx production in the polar atmosphere after recent powerful solar cosmic rays

E.A. Kasatkina¹, O.I. Shumilov¹, O.M. Raspopov², E. Kyro³, R. Kivi³

¹ Polar Geophysical Institute P.O. Box 162, 184209 Apatity, Russia

² St.-Petersburg Filial of IZMIRAN, P.O. Box 188, 191023 St.-Petersburg, Russia

³ Finnish Meteorological Institute, Sodankylä Department FIN-99600, Sodankylä, Finland

In the paper variations of NO₂ total content during large solar proton event of Ground Level Event (GLE) type (2 May 1998) are discussed. This GLE caused considerable stratospheric NO_x enhancement at high latitudes. Measurements of NO₂ were made by ground-based UV-visible spectrometer installed at Murmansk (68,58N, 33,03E). Increases of NO₂ slant column with maximum magnitude about 40% have been detected by this device. The results of model calculations showed significant NO₂ enhancement due to May 1998 GLE. Moreover, model results showed an ozone total content decrease (more than 10%) initiated by this GLE through additional NO_x production that seems contrary to experimental evidence.

The GLE of May 2, 1998 was very anisotropic one, and to investigate inhomogeneity of NO_x variations we've attracted nitrogen dioxide column measurements made at Sodankyla (67,20N, 26E). In analysis of meteorological situation during the event stratospheric temperature data were used.

In the paper the role of NO_x constituents in ozone destruction and validity of gas-phase photochemical theory in the light of our experimental results is discussed.

O4.5. Formation of atmospheric aerosols by cosmic rays and their possible influence on the climate

O.I. Shumilov¹, E.A. Kasatkina¹, O.M. Raspopov², K. Fadel³

¹ Polar Geophysical Institute, P.O. Box 162, 184209 Apatity, Russia

² St.-Petersburg Filial of IZMIRAN, P.O. Box 181, 191023 St.-Petersburg, Russia

³ Stockholm University, Kraftriket 24, 10691 Stockholm, Sweden

In this paper results of model calculations and measurements of atmospheric parameter changes after several GLEs (Ground Level Enhancements) of Solar Proton Events (SPE) are presented. We have got on lidar high-latitude measurements that after 16 February 1984 GLE event the increase of R(H) (backscattering ratio) at 17 km altitude reached 40%. The model calculations of CN (condensation nuclei) profile, which can be served as centers of sulfate aerosol and Polar Stratospheric Cloud (PSC) formation, demonstrate good coincidence with above-mentioned experimental data.

Besides, after other GLE event (2 May 1998) we measured considerable increase of NO (nitrogen dioxide) column of incident solar protons in polar region. All these data support the idea that aerosols created by galactic and solar cosmic rays may be one of the key factors in non-direct solar forcing mechanism influencing climate variability. These aerosols can block input of solar radiation to the Earth taking part in creation of additional cloudiness.

P4.1. Cloudiness and divergence between ground-based and satellite total ozone measurements

G. Milinevsky^{1,2}, M. Leonov², Z. Gritsai², ? . Evtushevsky², ? Katinas²

¹ Ukrainian Antarctic Center, 16, bv. Shevchenka, 01601 Kyiv, Ukraine

² Kyiv National Shevchenko University, 6, Glushkova, 05022 Kyiv, Ukraine

The comparison between ground-based and satellite total ozone data was provided for Antarctic region and Ukraine. Daily ozone values were selected separately for days with clear and total overcast sky. This allowed to analyse cloudiness influence on coincidence of ground-based and satellite measurement results. Data obtained in 1996-2000 by satellite EP/TOMS spectrometer, Dobson spectrophotometer at the Vernadsky Ukrainian Antarctic Station and ozonometer M-124 of the Kyiv University Lisnyky observatory were used. The better agreement is observed for the Vernadky Station in cloudy days (a relative TOMS-Dobson difference is negative: -0.7%), and for Lisnyky in cloudless days (relative TOMS - ? -124 difference is positive: 0.3%). Most disagreements were obtained for measurements into clear weather on Antarctic station (8.1%) and for cloudy weather on midlatitude station of north hemisphere (-4.3%). A determination of total ozone values by signal of satellite spectrometer is based on two limit levels, from which UV-radiation is receiving by device: from the Earth surface and from cloud cover. The local condition of the Earth surface and cloud cover is taking into account by suitable coefficients. From the disagreements obtained in this work follows that the TOMS calculations algorithm is more fitted for cloudy weather in Antarctic and to clear weather in middle latitudes of North hemisphere. The presented results indicate the possibility to correct data taking into account of cloudiness condition during satellite measurements.

P4.2. The changes of total ozone over Antarctic Peninsula and Ukraine for 1996-2001

G. Milinevsky^{1,2}, M. Leonov², Z. Gritsai², ? . Evtushevsky², V.Kravchenko ²

¹ Ukrainian Antarctic Center, 16, bv. Shevchenka, 01601 Kyiv, Ukraine

² Kyiv National Shevchenko University, 6, Glushkova, 05022 Kyiv, Ukraine

The ozone variations of the data obtained at Ukrainian Antarctic Vernadsky Station during six (1995/1996 - 2000/2001) ozone measurements seasons and at Ukraine at Lisnyky observatory in 1997-2000 are presented. At the Vernadsky Station the ozone measurements are provided by Dobson spectrophotometer N031. The total ozone data is obtained with relative accuracy about 1% during Direct Sun measurements and about 3% on Zenith Cloud measurements. The ozonometer M-124 type is used at Lisnyky observatory had been calibrated at the Vernadsky Station using Dobson spectrophotometer during 1997 winter over. Obtained relative measuring accuracy of M-124 is about 3% for Direct Sun measurements and 4-5% for Zenith Cloud measurements. The ozone changes during last years and reducing total ozone rate in two regions since 1970 years are discussed. In Antarctic region the reducing of total ozone took place with speed 7% for ten years. During 8 years (1994-2001) the stabilization of middle value about 265DU was observed. According satellite measurements (EP/TOMS) for Kyiv region the reducing total ozone rate is 1.9% for ten years. This rate is less, than ones observed in 40-65 North latitudes belt (- 4% according to WMO information).

P4.3. Invariability of total ozone content under solar proton events

V.C. Roldugin

Polar Geophysical Institute, Apatity, Russia

The changes of the total ozone content in the high-latitude point (65 N, 70 W geographic or 75 N, 12 E geomagnetic) is examined on TOMS' data for 19 solar proton events and for 21 Forbush decrease events. For both phenomena any statistical significant ozone changes are not revealed.

P4.4. Changes of atmospheric aerosol density after earth transits of the heliospheric current sheet

V.C. Roldugin¹ and **B.A. Tinsley²**

¹ Polar Geophysical Institute, Apatity, Russia.

² Center for Space Sciences, University of Texas at Dallas, Richardson, USA.

The variations of optical density of atmospheric aerosols in 369 nm, atmospheric spectral transparency in 530 nm and Junge index at 8 stations of Russian Ozonometric Network, situated to the North from 55 deg, were investigated by superposed epoch analyses for time interval 6 days before -6 days after heliospheric current sheet crossings. Two periods were chosen: 1983-1986 after El Chichon eruption, and 1978-1982 & 1987-1989 without volcanic activity. It was found that two days later HCS crossing the aerosol extinction decreases and the transparency increases for the Period of 1983-1986, and this effect does not take place for another period. We connect it with the decrease in relativistic electrons following the HCS crossing. The determining size of aerosols Junge index does not depend on HCS crossing, but it is smaller after El Chichon eruption. In 1983-1986 the transparency is higher and the aerosol extinction is smaller than in another period, that may be connected with solar activity effect

SESSION 5:
MESOSPHERIC AND THERMOSPHERIC PHYSICS

O5.1. Upper mesosphere/ lower thermosphere measurements by CRISTA (Invited)

Klaus U. Grossmann¹, Martin Kaufmann¹, Oleg Gusev¹, and Alexander Kutepov²

¹ University of Wuppertal, Dept. of Physics, 42097 Wuppertal, Germany

² Max-Planck-Institut für extraterrestrische Physik, 85748 Garching, Germany

During its two Shuttle missions in November 1994 and in August 1997 the Cryogenic Infrared Spectrometers and Telescopes for the Atmosphere (CRISTA) measured limb spectra in the mid- and far-infrared from the upper troposphere to the lower thermosphere. From the measured radiances temperatures and trace gas densities of CO₂, O₃, and atomic oxygen were retrieved using a non-LTE model in combination with a line by line radiative transfer code. Ozone concentrations for day and night are obtained up to about 95 km well into the secondary ozone maximum. CO₂ densities are derived for daytime only which was present over all of the northern hemisphere during the second CRISTA mission. Horizontal structures in the distribution of CO₂ agree qualitatively with the predictions of the TIME-GCM model. The CO₂ mixing ratios start to depart from their lower atmosphere values as low as 75-80 km. Temperatures derived from the CO₂ 15 μ m band reveal the very cold high latitude summer mesopause. Signatures from PMC were seen here by CRISTA as broadband thermal emission by mid-infrared and by far-infrared channels.

O5.2. Temperatures and semidiurnal tides in the mesopause region at 54°N and 28°N latitude by potassium lidar (Invited)

J. Oldag, J. Höffner, C. Fricke-Begemann, and U. von Zahn

Leibniz-Institute of Atmospheric Physics, Schloßstr. 6, D-18225 Kühlungsborn, Germany

During 1996 - 1998 the transportable IAP potassium lidar was operated at Kühlungsborn (54°N, 12°E) to provide a climatological series of nighttime temperature profiles at a midlatitude location. The measurements provide Doppler temperature profiles over the altitude range of the terrestrial potassium layer, that is between 78 to 110 km. The mesopause temperature exhibits clear evidence for the prevalence of a two-level structure. The mesopause is found to be located at a height of 100 km throughout the year, while during the summer season the mesopause occurs around 88 km. Additional observations obtained at Tenerife (28°N, 17°W) in 1999 and 2000 are in very good agreement with the concept of a global two-level structure of the mesopause. In addition the IAP potassium lidar measurements provide us an insight into the characteristics of thermal tides in the mesopause region. Monthly mean tidal variations of temperature from September to April are presented from our nocturnal lidar measurements at Kühlungsborn. Strong nighttime wave activity with downward phase progression was found according to upward-propagating tides over a height range of more than 20 km. Prominent semidiurnal tides were observed under winter conditions with monthly mean amplitudes reaching from 5 to 10 K at 100 km and vertical wavelengths from 23 to 45 km. At Tenerife monthly mean amplitudes of the semidiurnal tide in three summer months are 10 to 12 K at 100 km.

O5.3. Gravity Wave Measurements with a Near Infrared Scanning Radiometer at ALOMAR

Bob Lowe

Centre for Research in Earth and Space Technology and Department Physics & Astronomy The University of Western Ontario London, Canada

For several years, we have operated a near infrared scanning radiometer at the ALOMAR Observatory with the goal of characterizing the small-scale gravity wave climatology at this Arctic location and for correlative studies with other instruments located there. Identical instruments are in operation at our mid-latitude observatory in Canada and at Davis Station in Antarctica. The scanning radiometer takes a low resolution image of the overhead sky in the 1200 to 1600 nm. spectral region once permitted. A 1600 x 1600 degree field in the zenith is scanned with an instantaneous resolution of 1 degree. The airglow in the spectral region observed by the instrument is dominated by bands of the hydroxyl radical, though there is some contribution from oxygen bands during evening twilight. The instrument runs automatically whenever the sun is at least 6 degrees below the horizon.

The images obtained with the radiometer frequently show the signatures of small scale gravity waves that modulate the airglow intensity. In this paper we illustrate the analysis techniques used to extract gravity wave characteristics from the data and show examples of the seasonal variation in the direction and speed of propagation of waves observed at ALOMAR.

O5.4 Application of quantum-chemical approximations in the calculation of rate coefficients for intermolecular and intermolecular energy transfer processes of atmospheric gases

Andrei S. Kirillov

Polar Geophysical Institute, Apatity Murmansk region, 184200 Russia

Two-state models of the strong non-adiabatic coupling still play an important part in investigations of electron energy transfer in atom-molecular collisions. In such cases the main object of the theory of non-adiabatic processes consists in the explicit formulation of the 2x2 scattering matrix as a function of the parameters of the accepted model. An important assumption that is usually valid for low-energy collisions is that non-adiabatic coupling occurs only in effectively localized regions (so-called non-adiabatic regions), so that an explicit approximation of Hamiltonian matrix is needed only within these regions. We have paid a special attention to the application of Landau-Zener and Rosen-Zener models. The Landau-Zener model is formulated for a Hamiltonian with diagonal function linear in interatomic distance R and constant non-diagonal function. Rosen-Zener transition is a non-crossing near-resonant type in which two adiabatic states are parallel asymptotically. Rosen and Zener have found a solution of transition probability for a certain non-diagonal function. Obtained analytical expressions for the probabilities of electron energy transitions based on Landau-Zener and Rosen-Zener approximations have been suggested for the calculation of the coefficients of electron energy transfers in molecular collisions. The expressions of the coefficients could explain an exponential "energy gap" law in the behavior of measured coefficients in laboratory experiments. We consider coefficients of inelastic processes as the sum of the coefficients for intra- and intermolecular processes with small resonance defect. The calculations of rate coefficients have been made for collisions of molecular nitrogen, molecular oxygen and nitric oxide. The calculated coefficients for electron energy transfers have been compared with experimental data.

O5.5. Extreme Ultraviolet airglow. (Invited)

J.J. López-Moreno¹, M.J. López González¹, J.F. Gómez², C. Morales², S. Bowyer³, J. Edelstein³, E.J. Korpela³ and M. Lampton³.

¹ Instituto de Astrofísica de Andalucía, CSIC, Apdo. Correos 3004 18080 Granada, Spain

² Laboratorio de Astrofísica Espacial y Física Fundamental, INTA, Apdo. Correos 50727, E-28080 Madrid, Spain.

³ Space Science Laboratory, University of California, Berkeley, CA 94720-7304, USA

EURD (**E**spectrografo **U**ltravioleta extremo para la **R**adiación **D**ifusa) consists of two spectrographs that cover a bandpass from 350 to 1100 Å with 5 Å spectral resolution. The two spectrographs perform simultaneous observations with a field of view of 25°x 8°. The instrument is on board MINISAT01, a low orbit satellite launched the 21 April 1997 and still in operation and has accumulated more than 900 hours of observations in the Extreme Ultraviolet Nightglow. The orbit is circular at around 585 km with an inclination of 151°.

EURD has provided us with the most detailed atlas of the terrestrial UV nightglow never obtained. We present here the spectra obtained in both channels together with the identification of the lines, some of them identified for the first time in the nightglow. The spectra represent an improvement of various orders of magnitude with respect to the previous observation in terms of sensitivity. It has been possible the identification for the first time of the complete Lyman series of atomic hydrogen resolving up to Lyman-ε. It has also been possible to identify the helium Lyman-β line at 537 Å and the detection of other lines of the blended Lyman series of helium, at 515 and 522 Å. The spectra clearly show the presence of the OII lines at 617, 644, 673, 719, and 775 and 718 Å, previously observed in the dayglow but seen for the first time in the nightglow. In addition to the recombination continuum of the atomic oxygen OI at 911 Å two features of OI have been detected in the Nightglow the 3s-³D₀ transition at 989 Å, previously observed by Chakrabarti (1984) and a weak transition at 878 Å seen for the first time in the terrestrial nightglow.

O5.6. The Hydroxyl rotational temperature record from the Auroral Station in Adventdalen, Svalbard (78°N, 15°E): Preliminary results. (Invited)

F. Sigernes¹, K.P. Nielsen², C.S. Deehr³, T. Svenøe¹, N. Shumilov⁴, and O.Havnes⁴

¹ The University Courses on Svalbard, N-9171 Longyearbyen, Norway.

² The University of Bergen, Norway.

³ Geophysical Institute, University of Alaska Fairbanks, USA.

⁴ The Auroral Observatory, University of Tromsø, Norway

This paper describes the compiled mesospheric winter temperature series derived through over 20 years of ground - based spectral measurements of the hydroxyl airglow layer from the Auroral Station in Adventdalen near Longyearbyen, Svalbard (78°N, 15°E). Diurnal and semi diurnal tides are present. Amplitudes of 20 °K with extremes up to 70 °K within a few hours are usual. The average daily winter temperature for the period was found to be 206 °K with a standard deviation of 16 °K. In general the polar mesosphere has a winter warming, but no clear shapes or symmetry around solstice are observed from year to year. The temperature series is interspersed with periods of 2 - 5 days when the temperatures may drop as much as down to the summer minimum. These minima are probably associated with stratospheric warmings that occur with varying strength all winter. Some years are more quite than others with respect to variation in temperature. The annual mean winter temperatures show nearly zero temperature trend, indicating no observational change in the winter mesospheric temperatures over Svalbard during the last two decades.

O5.7. IR and thermal properties of mesospheric particles. (Invited)

Georg Witt

Department of Meteorology, Arrheniuslaboratoriet, Stockholm University, S-10691
Stockholm

TBD

O5.8. Polar cap disturbances: mesosphere and thermosphere – ionosphere response to solar - terrestrial interactions.

G. G. Sivjee and D. J. McEwen

Space Physics Research Laboratory Embry Riddle Aeronautical University, Daytona
Beach, Florida, USA.

The Polar Cap is the Upper Atmosphere cum Magnetosphere region, which is enclosed by the poleward boundary of the Auroral Oval and is threaded by open geomagnetic field lines. In this region, there is normally a steady precipitation (Polar Drizzle) of low energy (~ 100eV) electrons, which excite optical emissions from the ionosphere. At times, enhanced ionization patches are formed near the Dayside Cusp region, which drift across the Polar Cap towards the Night Sector of the Auroral Oval. Discrete auroral arcs and auroras formed during Solar Magnetic Cloud (SMC) / Coronal Mass Ejection (CME) events are also observed in the Polar Cap. Spectrophotometric observations of all these Polar Cap phenomena from the Arctic stations in Longyearbyen (79° N), Svalbard, Eureka (80° N) and Resolute Bay (76° N), Canada as well Sondrestromfjord (67° N), Greenland provide a measure of the average energy as well as energy flux of the electrons precipitating in the Polar Cap region during these disturbances. Such measurements also point to the Planetary, Tidal and Gravity Wave Modulations of the Polar Mesosphere-Lower Thermosphere (MLT) during six months long dark polar winters. Most of the Polar Cap MLT air density and temperature modulations appear to represent the effects of zonally symmetric tides whose Hough functions peak in the Polar region. MLT cooling during Stratospheric Warming events and their relation to Polar Vortex and associated Gravity wave activities are also observed at the Polar Cap sites. Results of optical remote sensing of these Polar Cap phenomena from the four Arctic stations are discussed.

O5.9. PMSE observed by 2.8 mhz radar during noctilucent clouds

V.C. Roldugin¹, V.D. Tereschenko¹, Ye.B. Vasilijev¹, S.M. Chernjakov¹ and S. Kirkwood²

¹Polar Geophysical Institute, Apatity, Russia

²Institute of Space Physics, Kiruna, Sweden

Visual, photographic and television observations of noctilucent clouds (NLC) over the partial reflection MF radar at Tumanny (69.0 N, 35.7 E) on 2.6-2.7 MHz have been observed during August 1999 and July - August 2000 from Uмба (Kola peninsula), Lekhta (Karelija) and Lycksele (Sweden). Nine events of NLC appearances of duration from 20 minutes to several hours were recorded. In all these cases the NLCs entail strong reflection of radar radiowave from 83-86 km altitude. The considerable depressions of electron concentration, "bite outs", are seen in the upper part of PMSE. The radar facility for the horizontal wind measurement shows in half cases some downward movements between 100 and 70 km at the velocity of 2 km/min. The ionosonde data in Loparskaya (68.6 N, 33.3 E) during NLC appearance are discussed. Analys of digital ionograms have shown that in the moment of appearance of PMSE and noctilucent clouds the intensive sporadic E-layers are observed.

O5.10. The non-lte problem for CO₂ in the middle and upper atmosphere: revision of radiative flux divergence

V.P. Ogibalov

Department of Atmospheric Physics, St.Petersburg State University, Ulyanovskaya 1, 198504 St.Petersburg-Petrodvorets, Russia

Radiative transfer in the IR vibrational-rotational bands of CO₂ under non-local thermodynamic equilibrium (non-LTE) conditions is an important factor in establishing the global heat balance, structure, and dynamical properties of the mesosphere and lower thermosphere (MLT) of Earth. Moreover, the emissions in the IR bands of CO₂ are used for remote sensing of the kinetic temperature and the CO₂ abundance in the MLT region. These reasons require both more sophisticated models of populations of the excited vibrational states of CO₂ and accurate radiative transfer schemes.

Using the modern data both on the abundances of CO₂ and atomic oxygen in the MLT region, values of the radiative flux divergence due to radiative transfer in the CO₂ vibrational bands have been revised for the layer 30–170 km. This based on: (1) use of the most detailed set of both the CO₂ vibrational states and the optical transitions between these states; (2) renewed rate constants for V–T and V–V processes; and (3) using a new algorithm which provides a high accuracy of the calculation! s. In particular, a new laboratory estimation of rate constant for the CO₂(v₂) mode quenching in collisions with atomic oxygen at temperatures within 200–300 K is used. Also, a new E–V mechanism of excitation of both the vibrational states of CO₂ and the N₂(1) and O₂(1) states is proposed. Revised values of radiative cooling rate in the CO₂ bands are investigated and compared with the previous ones.

For nighttime, it was for the first time shown that a contribution of the 4.3 μm CO₂ band to the total cooling can reach 0.2±0.35 K/day near the stratopause. For daytime, both the contribution of the CO₂ bands within the 15±1.05 μm spectral range to the total radiative flux divergence and its dependence on solar zenith angle have been investigated. It is shown that including the excitation mechanism O(¹D) + ng1033 → N₂(1) → CO₂(v₃) leads to an increase of cooling rate at the altitudes 80–120 km (with a maximum about 3 K/day at 105 km) mainly due to the 4.3 μm fundamental band of the principal isotope of CO₂.

P5.1. The study of the role of collisional processes in electronic kinetics of singlet and triplet states of molecular nitrogen in high-latitude upper and middle atmosphere

Andrei S. Kirillov

Polar Geophysical Institute, Apatity Murmansk region, 184200 Russia

The overall rate of the excitation of singlet and triplet states of molecular nitrogen in high-latitude atmosphere is comparable with the one of ion-electron pair production. The spontaneous transitions from the states cause the radiation of Vegard-Kaplan, First Positive, Lyman-Birge-Hopfield etc. band systems. The collisional quenching rates of the states are comparable with radiational ones in the region of middle atmosphere. Calculated according to Landau-Zener and Rosen-Zener approximations coefficients for intramolecular and intermolecular energy transfer processes between electronic states of molecular nitrogen have been used in the study of a role of collisional processes in electronic kinetics of the states at different altitudes of high-latitude atmosphere.

P5.2. A spectrum of atmospheric gravity waves in the mesosphere and thermosphere

V.M.Aushev¹, Ya.F. Ashkaliev¹, G.I. Gordienko¹, A.I. Pogoreltsev¹, V.V. Vodyannikov¹, A.F. Yakovets¹, R.H. Wiens²

¹ Institute of Ionosphere, Ministry of Education and Science, Almaty, 480020, Kazakhstan,

² Department of Physics, University of Asmara, Box 9556, Asmara, Eritrea, N.E. Africa

We present the results of simultaneous observations of acoustic gravity waves (AGWs) at the mesopause and traveling ionospheric disturbances (TIDs) in the F region of the ionosphere carried out since October 1997 till February 2001. AGWs spectra at the mesopause were obtained from fluctuations of the O₂ atmospheric (0-1) night airglow measured by the MORTI (Mesopause Oxygen Rotational Temperature Imager) instrument. AGWs spectra in the thermosphere were studied from fluctuations of virtual heights at series of sounding frequencies reflected from the bottom part of the ionospheric F2 region.

Two types of virtual height variations (periodical and quasi-stochastic) are found to exist in the thermosphere. The first one is related with AGWs identified by the downward direction of wave phase progression. The seasonal dependence of AGW presence is found. AGWs are presented during 70-85% of observations conducted in a period since October till March. In the summer, probability of their observations is only 20-40%. The rest part of observations revealed the quasi-stochastic character of virtual height variations.

Comparison of the intensity airglow variations at mesopause and virtual heights variations revealed their good correlation. Spectral analysis of these records showed a good coincidence of spectral peaks as well. Two groups of spectral peaks are found in the most spectra both for the mesopause and for thermospheric altitudes. Periods of the first group are ranged in 4-8 hours and centered on a period of 6 hours. This group is identified with the 3d-6th components of tidal oscillations in the atmospheric layers. The second group including periods of 0.7-3 hours is considered to be a manifestation of AGWs propagation. Vertical phase velocities of waves are determined from virtual height variations obtained for different sounding frequencies reflected from different altitudes. The phase velocities were found to increase when the period of a wave decreases. For low frequency spectral component with the average period of 6 hours an average velocity is found to be of 12.4 m/s. For the average period of 2.5 hours it equals to 21.1 m/s, and for the period of 1.6 hours it is 41.7 m/s.

In order to obtain an electron content variations amplitude as a function of the altitude, N(h) profiles are calculated. The absolute amplitude (ΔN) is shown to approach the maximum at altitudes located between a bottom of the F2 layer and its maximum. At the same time the relative amplitude ($\Delta N/N$) has maximum at the bottom of the F2 layer and gradually decreases up to the maximum of the layer.

SESSION 6:
TECHNIQUES, METHODS AND
INSTRUMENTATION

O6.1. Inversion of electron fluxes from all-sky images (Invited)

P. Janhunen

Finnish Meteorological Institute/GEO, Vuorikatu 15A, FIN-00100, Helsinki, Finland

Abstract: Inversion of precipitating electron fluxes from ground-based images has traditionally been carried out in two steps: one first inverts the 3D ionospheric photon volume emission rate for each measured wavelength using ordinary tomographic methods and then solves another inversion problem which contains a model for the emission physics to obtain the precipitating particle fluxes. We have developed a new approach in which the two steps are combined, i.e. the differential particle fluxes are inverted directly from the images. One of the advantages of the new approach is that the inversion is automatically restricted to physically possible volume emission rate profiles, thus making it unnecessary to invent extra a priori conditions. Another advantage is that the method is capable of producing reasonable results (errors not larger than the inherent uncertainties in the emission physics modeling) even when the number of available images is small and weather conditions imperfect. The method has been implemented in an easy to use program that currently is set up to work for FMI/GEO all-sky camera data. One inversion takes from some tens of seconds to a few minutes, depending on the resolution wanted and the number of images and wavelengths available.

O6.2. New method for study of aurora brightness spatial distribution

Arinin V. A.¹ and Tagirov V.R.²

¹ Institute of Explosion Physics, Russian Federal Nuclear Center, 607190, Sarov, Russia.

² Polar Geophysical Institute, Russian Academy of Sciences, 184200, Apatity, Russia.

The proposed method for study of spatial distribution of brightness of auroral phenomena and another optical luminous objects in the atmosphere is based on direct one-pass geometrical conversion of an image obtained by all-sky TV camera. The conversion removes all types of geometrical distortions, such as distortions due to fish-eye camera optics, non-linearity of TV raster, inclination and incorrect turn of camera, etc. The main idea of the one-pass method was to exclude transitory stages in processing of auroral data, such as determination of distortion curves, which proposes that the image is center symmetrical. This was made by using the method of Gouraud network. The network and corresponding vector field for correction of the image was constructed on the basis of position of stars on TV image. The usage of special algorithms during processing of video data permits to obtain coordinates of the stars with sub-pixel accuracy. Finally, to determine auroral forms at particular height we used complimentary colors to paint corrected auroral images from each observational point projected onto geographical grid. Those auroral forms, which fit together at proposed altitude, get the white color. The triangulation of any objects with usage of arbitrary quantity of observational points is possible. Alongside with auroral phenomena the triangulation measurements could be made for another atmospheric luminous objects, for example, we present the results of triangulation of large meteorite trajectory.

O6.3. Can computers understand auroral images?

M.T Syrjäsuo¹, E.F. Donovan² and L.L. Cogger²

¹ Finnish Meteorological Institute / Geophysical Research, Vuorikatu 15 A 3, FIN-00100 Helsinki

² Department of Physics and Astronomy, University of Calgary, Calgary, Alberta, Canada

The aurora provides us information about processes in the magnetosphere and the ionosphere. Today's auroral research utilizes sensitive auroral all-sky cameras (ASC) that capture the whole sky in one image. These cameras produce millions of images every year, which makes it difficult to search for events systematically and objectively. We present techniques that can be used to classify all-sky images automatically into those containing aurora and those without apparent auroral luminosity. We demonstrate that in the case of CANOPUS ASC data an accuracy of about 90% can be achieved. Classification results from MIRACLE data are also presented. As well, we demonstrate arc tracking and the retrieval of similar images from database.

O6.4. A new spectrograph platform for auroral studies in Svalbard

I. McWhirter¹, I. Furniss¹, A.D. Aylward¹; B.S.Lanchester², M.H. Rees², S.C. Robertson²

¹ Atmospheric Physics Laboratory, University College London, 67-73 Riding House Street, London W1P 7PP, UK.

² Department of Solar Terrestrial Physics, University of Southampton, UK.

A versatile spectrograph platform has been installed by University College London at the Adventdalen Observatory in Svalbard. The platform was primarily built to support the Southampton University study of proton aurora and small-scale auroral features. It has successfully recorded the spectral profile of the Doppler broadened H-beta emission line (486.1 nm) and observed the predicted red-shifted component due to proton back-scatter. The platform consists of a HITIES (High Throughput Imaging Echelle Spectrograph) manufactured by Boston University, together with two photon-counting photometers built by UCL and a narrow-field intensified video camera. All instruments are co-aligned and centred on the magnetic zenith. This combination of instruments can discriminate between spatial and temporal variations of small-scale features and thus complements measurements by narrow beam radar, which is unable to do this. The system can be controlled remotely over the Internet.

O6.5. Development of an Online Field Aligned Support Imager for the ESR.

Stuart Robertson

Marie Curie Scholarship student at University of Oulu, Department of physical sciences,
P. O. Box 3000, FIN-90014 University of Oulu

A report on the construction of an online imager to support the ESR. The Camera, located at Nordlysstation, resolves a 12° by 16° section of sky in the field-aligned direction. The project involves bringing this camera online and the development of innovative web based video-radar data correlation methods. Plus a note on using calibrated stars to calibrate instrument intensity response.

O6.6. Application of the I-PentaMAX CCD camera for auroral observations

L.Borovkov and **S.Chernouss**

Polar Geophysical Institute of the Kola Science Centre of Russian Academy of Sciences, 14 Fersman str., Apatity 184200 Russia

The I-PentaMAX -512EFT CCD camera was tested as a tool for auroral researches in field conditions at Apatity, Kola peninsula. The intensified digital CCD camera system was used both for auroral image and auroral spectra observations. The advantages of high dynamic range (12 bits) and high sensitivity are discussed. The auroral spectra of the main auroral emissions obtained by Imagine Spectrograph are demonstrated. Application of the camera system for measurements of Doppler shift of optical emission by the Fabry-Perot interferometer permits to use rather short exposures (tens of seconds).

Method of spectral resolution improvement by order (up to 0.01 nm) is suggested and discussed.

O6.7. DIAL measurements of stratospheric ozone.

M. Gausa¹, U.-P. Hoppe² and G.H. Hansen³

¹ ALOMAR, Andøya Rocketrange, Postbox 54, N-8483 Andenes, Norway

² Norwegian Defence Research Establishment (FFI), N-2027 Kjeller, Norway

³ Polarmiljøsentret, N-9296 Tromsø, Norway

The capabilities of the ALOMAR Ozone Lidar to measure stratospheric ozone profiles in the daylight have been much improved since the 27 AM. We will present the nature of the improvements and data collected in daylight.

O6.8. Bistatic stereoscopy in studies of polar stratospheric clouds

Carl-Fredrik Enell¹, Björn Gustavsson¹, Kerstin Stebel¹, Ulrich Blum², Urban Brändström¹, Karl-Heinrich Fricke², Sheila Kirkwood¹ and Åke Steen³

¹ Institutet för rymdfysik, Box 812, SE-98128 Kiruna

² Physikalisches Institut, Universität Bonn, Nußallee 12, D-53115 Bonn

³ RemSpace Group, Rekrytgatan 2, SE-58214 Linköping

Polar stratospheric clouds (PSCs) have been studied with photographic methods at least since the beginning of last century. After the recognition of the large chemical ozone depletion in the Antarctic and Arctic spring stratospheres, it turned out that PSCs are not a mere curiosity but an important part of stratospheric chemistry. It has been argued that the uncertainty in PSC coverage caused by local generation of PSCs in mountain-induced waves is a reason for the discrepancy between modelled and observed ozone depletion. It is therefore desirable to collect all PSC observations available into an observational PSC climatology.

However, historical observations of PSCs are mainly limited to the so-called mother-of-pearl or nacreous clouds, which are characterised by their conspicuous iridescent appearance. It is not entirely clear which types of PSC that show the mother-of-pearl appearance. For interpretation of the observations a better understanding of the optical appearance of PSCs under different dynamic conditions is needed. Tracking of nacreous clouds with multistatic imaging methods and coordinated lidar studies provides a method to settle these questions. In this talk methods for semi-automatic stereoscopy of mother-of-pearl clouds and their application will be discussed.

O6.9. Ground based instrumentation at Esrange

Ola Widell

Swedish Space Corporation, Esrange, P.O. Box 802, SE-98128 Kiruna, Sweden,
Tel: +46 980 720 00, fax: +46 980 12890.

This is a review of the latest improvements made at Esrange for scientific ground based instrumentation.

The ESRAD MST radar at Esrange has been upgraded during year 2000. The antenna array is extended and new feeder cables make the radar more sensitive and the radiated power has increased. ESRAD is operated jointly by the Swedish Institute of Space Physics and the Swedish Space Corporation at Esrange. ESRAD is a 52 MHz MST class radar that has been in near continuous operation since the middle of 1996. A new optical platform called KEOPS is established. The KEOPS facility is located 1.5 km west of the Esrange Rocket Range on a mountain at 530m altitude. KEOPS is an excellent site for optical ground based instruments with possible remote interaction by use of Internet.

Esrange geographical location 68° N and 21°E on the eastern side of the Scandinavian Mountains is a ideal site for studying interesting scientific phenomena's like stratospheric waves and PSC clouds.

O6.10. Optical auroral instrumentation of University of Oulu

J. Jussila, H. Holma and K. Kaila

Department of physical sciences, P.O. Box 3000, FIN-90014 University of Oulu, Finland

Space physics group of University of Oulu is making optical auroral measurements with several different kinds of instruments and in several locations. Instrumentation consists of photometers and cameras. Also spectrometers have been developed. Used locations in Northern Scandinavia are Kilpisjärvi (69,02°N, 20,87°E), Karesuvanto (68,47°N, 22,44°E) and Sodankylä (67,42°N, 26,39°E). Tromsø EISCAT site at Ramfjordmoen (69,59°N, 19,23°E) is used during EISCAT campaigns. Some instruments have also been used in IRF-Kiruna and Esrange, in Sweden. A photometer is also been used in Chinese Zhong Shan station in Antarctic since 1996.

Used photometers have 5 or 6 measurement channels. These are 557.7 nm (O^1S), 630.0 nm (O^1D), 427.8 nm (N^{2+} band), 427.0 nm (N^{2+} band), 428,6 nm (N^{2+} band) and 486.0 nm (proton band). Half bandwidth of used interference filters is 2 nm. Backgrounds of measured emissions are measured by tilting the filter. Normally this is done after every 15 minutes. In three photometers proton channel is equipped with swinging filter, to cover the whole proton band. Field-of-view (FOV) varies from 0.5 degrees to 3 degrees. Photometers can be used in scanning or fixed mode. Also a combination of these is possible. Maximum sampling resolution is 1 ms.

Both real-speed and snapshot cameras are used. The real-speed cameras use European standard of 25 frames/s. All the cameras have changeable optics, allowing different kind of FOVs. Nowadays a FOV of 50 degrees is used. One of the cameras has possibility to use interference filters, but most of the recording are made in white light, i.e. without filters. Due to this, recordings are not made during full moon. Older cameras are ISIT-based and new cameras have CCD-based detectors. Used new snapshot camera is based on high quantum efficiency back illuminated CCD-chip. Structures and measurement modes of the instruments and data samples are presented. Also some future plans are presented.

O6.11. OPTICS at the Auroral Station in Adventdalen, Svalbard

Fred Sigernes¹, Trond Svenøe¹ and Charles Deehr²

¹ The University Courses on Svalbard, N-9171 Longyearbyen, Norway;

² Geophysical Institute, University of Alaska, Fairbanks, Alaska, U.S.A.

This paper describes the Auroral Station in Adventdalen near Longyearbyen, Svalbard (78°N, 15°E). The main instruments at the site are for optical observation of aurora and airglow, but magnetic and radar observations are also carried out. Emission spectra show the difference between the day- and night side optical aurora. The newly compiled mesospheric temperature series derived through 20 years of spectral measurements of the hydroxyl airglow layer shows no observational change in the atmospheric temperatures of the upper polar atmosphere during that period.

P6.1. Lossy compression of scientific images of aurora

Peter Rydesäter¹, Björn Gustavsson², Urban Brändström², Carl-Fredrik Enell², Åke Steen³

¹ Mitthögskolan, 83125 Östersund, Sweden

² Institutet för rymdfysik, Box 812, SE-98128 Kiruna

³ RemSpace Group, Rekrytgatan 2, SE-58214 Linköping

Abstract: Digital storage and transmission of scientific images can be demanding due to the amount of data. Lossless compression of data often gives poor compression, especially when the data consists of a considerable amount of noise. Lossy compression of scientific data is unusual, probably because it is not known how it impacts on the results of further analysis of the data. In this work, images of aurora observed with the ALIS measurement system are used to verify how lossy compression impacts on the results. The error from lossy compression is compared to measurement noise, and we found that it is similar and of an acceptable level for many analysis applications of the data.

P6.2. Thermospheric neutral temperature measurements from the University College London Fabry-Perot interferometers

I. McWhirter

Atmospheric Physics Laboratory, University College London, 67-73 Riding House Street, London W1P 7PP, UK.

The ionosphere responds almost immediately to magnetospheric forcing, however, the neutral atmosphere has inertia owing to its far greater mass density. As a consequence the neutral atmosphere can significantly modify the ionosphere-magnetosphere coupling processes such as the energy transferred between them. Thermospheric neutral temperatures measured by FPI from airglow are presented from both auroral and polar cap sites. These are compared to both ISR derived values and modeled temperatures from MSIS. The large differences evident in the comparison to model results are discussed and the reaction of the measured values to geomagnetic conditions are demonstrated from both sites. We demonstrate the importance of accurate neutral temperatures in monitoring the dissipation of energy and in the derivation of ionospheric parameters.

SESSION 7:
CALIBRATION

O7.1. All-sky camera calibration

S. Mäkinen

Finnish Meteorological Institute, Vuorikatu 15 A, FIN-00101 Helsinki, Finland

All-sky cameras are used to monitor the auroral forms and the motion of larger-scale structures. All-sky camera consists of an optical system, a CCD camera and a control system that controls an image intensifier, a mechanical shutter and a filterwheel. All-sky cameras use fish-eye lenses to acquire an image of the whole sky in one shot. The control system and the CCD camera is controlled by a computer. In order to be able to scale the recorded intensities of different cameras to same reference levels, the cameras have to be calibrated. A calibrated light source has to be used. The all-sky cameras include narrow band interference filters. The filter transmission curves have to be known.

O7.2. Calibration of an Auroral Large Imaging System

U. Brändström¹, B. Gustavsson¹, C-F. Enell¹, T. Aso², M. Ejiri² and Å. Steen³

¹ Swedish Institute of Space Physics, Box 812, SE-981 28 Kiruna, Sweden

² National Institute of Polar Research, NIPR, Itabashi, Tokyo 173-8515, Japan

³ RemSpace Group, Rekrytgatan 2, SE-582 14 Linköping, Sweden

We will present calibration procedures for the monochromatic CCD-imagers used in the Auroral Large Imaging System. Current project status and highlights from ALIS measurements will also be presented.

P7.1. Absolute optical calibrations using a simple tungsten bulb: theory

O. Harang¹ and **M. J. Kosch**²

¹ Nordlysobservatoriet, University of Tromsø, Norway

² Communication Systems, University of Lancaster, LA1 4YR Lancaster, UK

The absolute spectral intensity calibration of optical detectors has always been difficult. In the past, this was only possible using expensive sources, which had been cross-calibrated against national standards. We describe a simple theoretical approach to absolute optical calibrations using any ordinary Tungsten light bulb. A key element of the theory is transforming Tungsten into an equivalent black body radiator. This permits direct application of Boltzmann's and Planck's formulas of radiation.

AUTHORS AND PARTICIPANTS OF THE 28TH OPTICAL MEETING

Aikio, Anita	University of Oulu	Finland	Anita.Aikio@oulu.fi
Amm, Olaf	Finnish Meteorological Institute	Finland	Olaf.Amm@fmi.fi
Arinin, Vladimir	Russian Federal Nuclear Center	Russia	root@gdd.vniief.ru
Aushev, V.M.	Institute of Ionosphere, Ministry of Education and Science	Kazakhstan	aush@ionos.alma-ata.su
Belikov, Yu.E.	Fedorov Institute of Applied Geophysics	Russia	geophys@hydromet.ru
Brändström, Urban	Swedish Institute of Space Physics	Sweden	urban.brandstrom@irf.se
Chernouss, Sergey	Polar Geophysical Institute	Russia	chernouss@pgi.kolasc.net.ru
Danielides, Michael	University of Oulu	Finland	Michael.Danielides@oulu.fi
Degenstein, Doug	University of Saskatchewan	Canada	degenstein@irg.usask.ca
Didebulidze, G. G.	Abastumani Astrophysical Observatory	Georgia	didebulidze@yahoo.com
Donovan, Eric	University of Calgary	Canada	eric@phys.ucalgary.ca
Enell, Carl-Fredrik	Swedish Institute of Space Physics	Sweden	carl-fredrik.enell@irf.se
Gausa, Michael	Andøya Rocket Range	Norway	michael.gausa@rocketrange.no
Grossmann, Klaus U.	University of Wuppertal	Germany	gross@wpos2.physik.uni-wuppertal.de
Henricson, Hans	Swedish Space Corporation	Sweden	hans.henricson@esrange.ssc.se
Holma, Hannu	University of Oulu	Finland	Hannu.Holma@oulu.fi
Janhunen, Pekka	Finnish Meteorological Institute	Finland	pekka.janhunen@fmi.fi
Jussila, Jouni	University of Oulu	Finland	Jouni.Jussila@oulu.fi
Kaila, Kari	University of Oulu	Finland	Kari.Kaila@oulu.fi
Kangas, Jorma	Sodankylä Geophysical Observatory	Finland	Jorma.Kangas@sgo.fi
Kasatkina, Elena A.	Polar Geophysical Institute	Russia	oleg@aprec.ru
Kauristie, Kirsti	Finnish Meteorological Institute	Finland	kirsti.kauristie@fmi.fi
Kirillov, Andrei S.	Polar Geophysical Institute	Russia	kirillov@pgi.kolasc.net.ru
Kornilov, Iliia A.	Polar Geophysical Institute	Russia	kornilov@pgi.kolasc.net.ru
Kornilova, Tatiana	Polar Geophysical Institute	Russia	kornilova@pgi.kolasc.net.ru
Kosch, Michael	Lancaster University	UK	m.kosch@lancaster.ac.uk
Kozelov, Boris V.	Polar Geophysical Institute	Russia	kozlov@pgi.kolasc.net.ru
Kozlovsky, Alexander	University of Oulu	Finland	Alexander.Kozlovsky@oulu.fi
Laine, Unto	Helsinki University of Technology	Finland	Unto.Laine@hut.fi
Lakkala, Timo	Sodankylä Geophysical Observatory	Finland	Timo.Lakkala@ramk.fi
Leontyev, Sergej V.	Polar Geophysical Institute	Russia	leontyev@pgi.kolasc.net.ru
Leppelmeier, Gilbert W.	Finnish Meteorological Institute	Finland	gilbert.leppelmeier@fmi.fi
Llewellyn, Edward J.	University of Saskatchewan	Canada	llewellyn@dansas.usask.ca
López-Moreno, Jose Juan	Instituto de Astrofísica de Andalucía	Spain	lopez@iaa.es
Lowe, Bob	The University of Western Ontario	Canada	lowe@physics.uwo.ca
Lummerzheim, Dirk	University of Alaska	USA	lumm@gi.alaska.edu

Lyatsky, Wladislaw	University of New Brunswick Polar Geophysical Institute	Canada Russia	lyatsky@unb.ca
Manninen, Jyrki	Sodankylä Geophysical Observatory	Finland	Jyrki.Manninen@sgo.fi
McWhirter, Ian	University College London	UK	ian@apg.ph.ucl.ac.uk
Milnevsky, Gennadi	Ukrainian Antarctic Center	Ukraine	atarc@carrier.kiev.ua
Moen, Jöran	University of Oslo	Norway	jmoen@fys.uio.no
Mursula, Kalevi	University of Oulu	Finland	Kalevi.mursula@oulu.fi
Murtagh, Donal	Chalmers University of Technology	Sweden	donal@rss.chalmers.se
Mäkinen, Sanna	Finnish Meteorological Institute	Finland	Sanna.Makinen@fmi.fi
Nicholson, Natalya	University of Calgary	Canada	natalya@phys.ucalgary.ca
Nygrén, Tuomo	University of Oulu	Finland	Tuomo.Nygren@oulu.fi
Ogibalov, Vladimir P.	St. Petersburg State University	Russia	vpo@lmupa.phys.spbu.ru
Oikarinen, Antti	University of Oulu	Finland	Antti.Oikarinen@oulu.fi
Oldag, Joern	Leibniz Institute of Atmospheric Physics	Germany	oldag@iap-kborn.de
Penttinen, Krista	University of Oulu	Finland	krpentti@mail.student.oulu.fi
Pitkänen, Veli	University of Oulu	Finland	vtpitkan@student.oulu.fi
Robertson, Stuart	University of Southampton	UK	scr@phys.soton.ac.uk
Roldugin, V.C.	Polar Geophysical Institute	Russia	roldugin@pgi.kolasc.net.ru
Rydesäter, Peter	Mitthögskolan	Sweden	Peter.Rydesater@mh.se
Safargaleev, Vladimir	Polar Geophysical Institute	Russia	safar@pgi.kolasc.net.ru
Sergienko, Tima	Swedish Institute of Space Physics	Sweden	time@irf.se
Shumilov, Oleg I.	Polar Geophysical Institute	Russia	oleg@aprec.ru
Sigernes, Fred	University Courses on Svalbard	Norway	fred@unis.no
Sivjee, Gulamabas G.	Embry Riddle Aeronautical University	USA	sivjee@db.erau.edu
Starkov, Guenrikh	Polar Geophysical Institute	Russia	starkov@pgi.kolasc.net.ru
Syrjäsuu, Mikko T.	Finnish Meteorological Institute	Finland	Mikko.Syrjasuu@fmi.fi
Tagirov, Vartan	Polar Geophysical Institute	Russia	tagirov@pgi.kolasc.net.ru
Turunen, Esa	Sodankylä Geophysical Observatory	Finland	Esa.Turunen@sgo.fi
Ulich, Thomas	Sodankylä Geophysical Observatory	Finland	Thomas.Ulich@sgo.fi
Widell, Ola	Swedish Space Corporation	Sweden	ola.widell@esrange.ssc.se
Witt, Georg	MISU	Sweden	gwitt@misu.su.se
Yahnin, Alexander G.	Polar Geophysical Institute	Russia	yahnin@pgi.kolasc.net.ru

INFORMATION

1. PAPERS

Oral and poster papers will be presented on Monday to Thursday in scientific sessions. Special requirements like data projector have to be indicated beforehand. Invited talks are 30 minutes (25+5), others 20 minutes (15+5).

Poster stands will be 90 cm (width) * 100 cm (height). Posters will be available during the whole week without any special poster session.

2. PROCEEDINGS

Proceedings of the 28AM will be published at the Sodankylä Geophysical Observatory Publications. It will be refereed. Invited papers will have a limit of six (6) pages and regular papers four (4) pages. Papers may include colour pages, but there will be 50 EUR fee per colour page.

Papers must be submitted in LaTeX-format. Instructions can be found from <http://spaceweb.oulu.fi/28AM/proceedings.html>.

Timetable for proceedings:

- 31.11.2001: Deadline for submitting manuscripts
- 1.3.2002: Referees' reports to authors
- 1.5.2002: Submission of camera-ready articles
- June 2002 Publication of proceedings

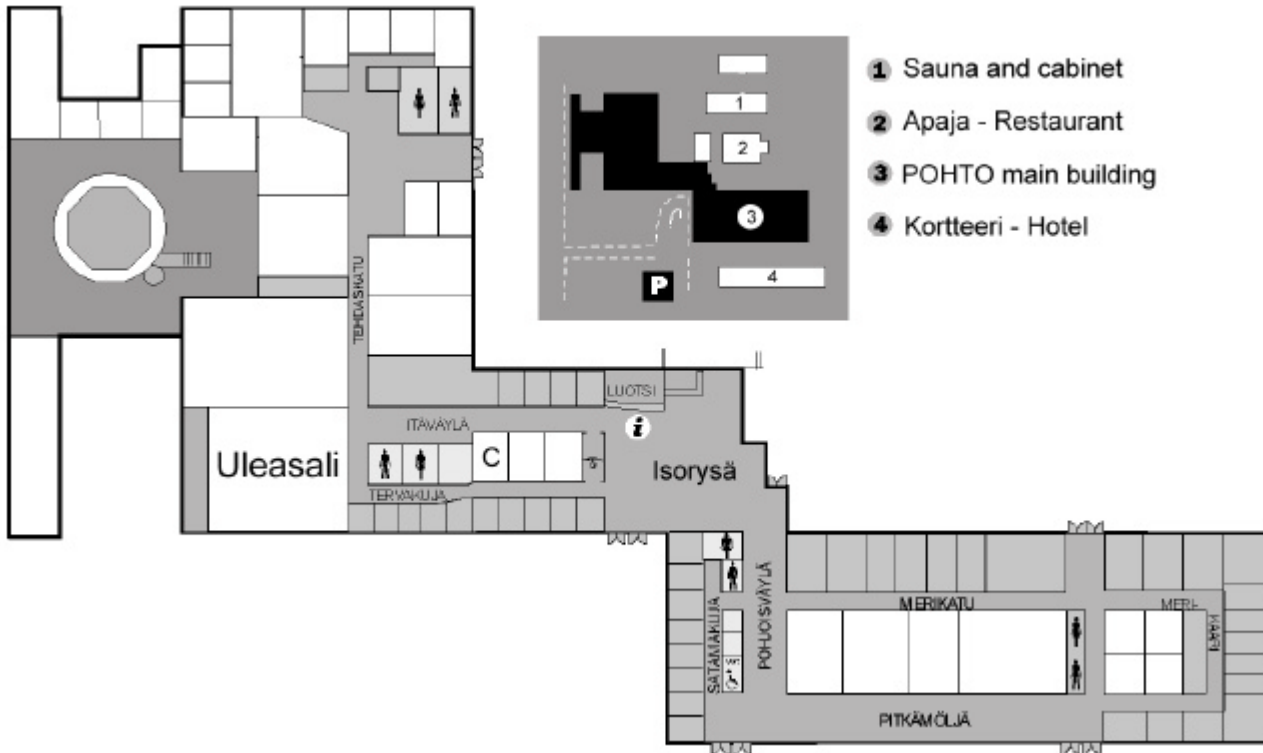
3. DINING

Lunches at the meeting place will cost 11 EUR / 65 FIM. Payment with lunch tickets which has to be paid in advance with conference fee or at conference desk on arrival.

Coffee break twice a day, included in the conference fee.

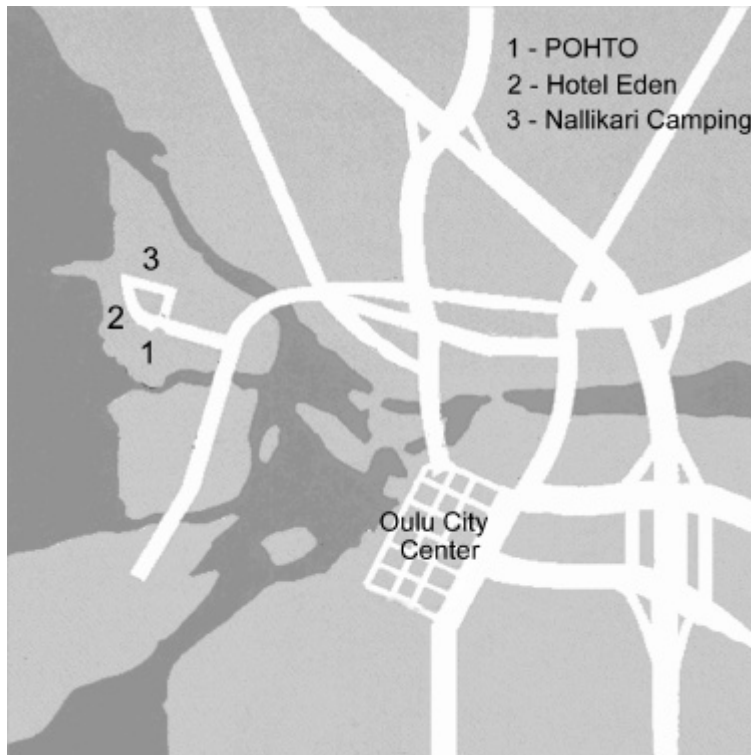
4. THE MEETING PLACE

The meeting will be held at POHTO (The Institute for Management and technological Training, Vellamontie 12). POHTO is a conference and training center located on the seashore on an island (Hietasaari) between Baltic Sea and river Oulujoki. The distance to the center of the city is 3 km through parks and along walking bridges over the river and 4.5 km by car.



The Floor plan of the meeting place. Meeting is taken place in "Uleasali", Coffees and registration in "Isorysä" and lunch in "Apaja" -restaurant. The Icebreaker and the conference sauna will take place in Cabinet.

5. MEETING PLACE LOCATION



6. PHONE NUMBERS:

Emergency calls:

Fire/Ambulance: 112

Police: 10022

Addresses and telephone numbers: 118

Taxi: +358 (0)100 4181

Spa hotel Eden: +358 (0)8 5504 100

Pohto: +358 (0)8 5509 700

Nallikari camping: +358 (0)8 558 61350 / +358 (0)8 558 61351

7. SOCIAL PROGRAMME

- Excursion to Oulu and Kierikki archeological center on Sunday 19.8. Starting at 11.00 at POHTO
- Icebreaker sauna on Sunday 19.8. evening at POHTO. Starting at 19.00.
- Conference sauna on Tuesday 21.8. Starting at 19.00.
- Conference dinner on Wednesday 22.8. Transportation starting at 19.00 at POHTO

8. BUS ROUTES:

Bus number 5 goes between City center and Hietasaari, where meeting takes place. Timetables are as following:

Bus no. 5: Hietasaari – City center (~10 min)			
hours	Minutes		
	Monday to Friday	Saturday	Sunday
8	00		
9	00		
10	00	00	
11	00	00	
12	00	00	00
13	00	00	00
14	00	00	00
15	00	00	00
16	00	00	00
17	00	00	00
18	00	00	00
19	00	00	
20	00	00	
21	00	00	

Bus no. 5: City center – Hietasaari (~10 min)			
Hours	Minutes		
	Monday to Friday	Saturday	Sunday
7	45		
8	45		
9	45	45	
10	45	45	
11	45	45	45
12	45	45	45
13	45	45	45
14	45	45	45
15	45	45	45
16	45	45	45
17	45	45	45
18	45	45	
19	45	45	
20	45	45	

Bus number 19 goes between City center and Airport. Timetables are as following:

Bus no. 19: Airport – City center (~25 min)					
hours	Minutes				
	Monday to Friday			Saturday	Sunday
6	00				
7	05	25	45		
8	05	25	45	25	
9	05	25	45	25	
10	05	25	45	25	25
11	05	25	45	25	25
12	05	25	45	25	25
13	05	25	45	25	25
14	05	25	45	25	25
15	05	25	45	25	25
16	05	25	45	25	25
17	05	25	45	25	25
18	05	25	45	25	25
19	15		45	25	25
20	15		45	25	25
21	15		45	25	25
22			45	45	45
23			45	45	45
00					
01	15			15	15

Bus no. 19: City center – Airport (~25 min)					
Hours	Minutes				
	Monday to Friday			Saturday	Sunday
6	10		35		
7	05	25	45	40	
8	05	25	45	40	
9	05	25	45	40	40
10	05	25	45	40	40
11	05	25	45	40	40
12	05	25	45	40	40
13	05	25	45	40	40
14	05	25	45	40	40
15	05	25	45	40	40
16	05	25	45	40	40
17	05	25	45	40	40
18	00	30		40	40
19	00	30		40	40
20	00	30		40	40
21	00	30		40	40
22	00		50	50	50
23					
00			50	50	50
01					